ELSEVIER

Chemical Engineering Journal 138 (2008) 556–577

Chemical Engineering Journal

www.elsevier.com/locate/cej

Modeling, simulation and optimization: Mono pressure nitric acid process

I.B. Chatterjee, J.B. Joshi *

Institute of Chemical Technology, University of Mumbai, Matunga, Mumbai 400 019, India

Received 18 March 2007; received in revised form 12 July 2007; accepted 13 July 2007

Abstract

The present work focuses on a strategy for optimizing mono pressure weak nitric acid plants. The optimization strategy addresses important processes which include oxidation of ammonia to nitric oxide, heat recovery from product stream of ammonia oxidation reactor and absorption accompanied by complex chemical reactions of multi-component nitrogen oxide gases into water. In design and optimization of nitric acid process, it is essential to understand the rate controlling step for ammonia oxidation process, strategy to be adopted for heat exchanger network design, rates of mass transfer and chemical reaction for nitrogen oxide absorption and the combined effects of several equilibria. The work addresses these issues taking through the complexities in the above mentioned processes.

The parametric sensitivity of few parameters such as ammonia to air ratio, excess oxygen/air, selectivity, power recovery based on the performance efficiency of compressor and expander, inlet and outlet nitrogen oxide composition in condenser and absorption column have been a part of our investigation either explicitly or implicitly. Further, for the absorption column, the effects of geometrical parameters, excess air, extent of absorption, product acid concentration, temperature and pressure have been analyzed for the purpose of optimization of nitric acid plant. All parameters having major influence on annualized cost of product acid have been analyzed and presented.

Keywords: Nitric acid manufacture; Optimization strategy; Ammonia oxidation; Platinum losses; Multi-component absorption; NO*x* absorption; HNO_3 tray profiles

1. Introduction

In making nitric acid, as in most other products, there is no single "right way". It would be difficult to cite a process so common to industrial chemical scenario and yet posing so severe a challenge to our comprehension of its fundamental mechanism as that of absorption of nitrogen oxides in water to produce nitric acid. The manufacture of nitric acid process comprises of oxidation of ammonia to produce nitrogen oxides, followed by gas phase oxidation of nitric oxide by oxygen, and subsequent absorption and reaction of the higher nitrogen oxides into water to produce nitric acid. In this work the focus is on mono high pressure processes. A typical process flow diagram is presented in Fig. 1 [1].

In a mono high pressure process, the absorption column plays a dual role: (a) HNO_3 manufacture and concurrently (b) NO*x* abatement. Hence, the understanding of the mechanism of NO*x* absorption holds the key to nitric acid manufacture. Considerable research efforts have been expended [2–7] to bring out the following aspects of NO*x* absorption: (i) NO*x* gases consists of several components NO, NO_2, N_2O_3, N_2O_4, HNO_2, HNO_3, etc. and the liquid phase contains two oxyacids (i.e. nitric acid and nitrous acid), (ii) several reversible and irreversible reactions occur both in gas and liquid phases, (iii) absorption of multiple gases is accompanied by chemical reaction, (iv) desorption of gases occur preceded by chemical reaction, (v) heterogeneous equilibria prevail between the gas and the liquid phase components, (vi) heat effects of the absorptions and the chemical reactions. All these aspects make the process of NO*x* absorption probably the most complex with respect to other absorption operations.

In addition to these attempts made in the past [8–10], the following important features have been considered in the present model for absorber. (i) The rates of absorption of NO_2, N_2O_3 and N_2O_4 in nitric acid are different from those in water. The rates decrease with an increase in concentration of nitric acid. (ii) Carberry [11] in his work has shown that, for a given set of partial pressures of NO, NO_2 and N_2O_4, there exists a certain limiting concentration of nitric acid beyond which no absorption of either N_2O_4 or NO_2 occurs. This heterogeneous equilibrium substantially reduces the rates of absorption of NO_2, N_2O_3 and

* Corresponding author. Tel.: +91 22 414 5616; fax: +91 22 414 5614.
E-mail address: jbj@udct.org (J.B. Joshi).

1385-8947/$ – see front matter © 2007 Elsevier B.V. All rights reserved.
doi:10.1016/j.cej.2007.07.064

Nomenclature

$\hat{a}$	wire area per gauze cross sectional area ($m^2\ m^{-2}$)
$\underline{a}$	surface area per unit volume ($m^2\ m^{-3}$)
C_i	concentration for species i ($kmol\ m^{-3}$)
D	diameter (m)
e	efficiency
f	friction factor
F_i	molar flow rate for species i ($kmol\ s^{-1}$)
g	acceleration due to gravity ($m\ s^{-2}$)
G	inert molar flow rate ($kmol\ s^{-1}$)
H	height of column (m)
k	mass transfer coefficient ($m\ s^{-1}$)
k_b	backward rate constant for reaction Eq. (5) ($kmol\ kN^{-1}\ s^{-1}$)
k_f	forward rate constant for reaction Eq. (5) ($kmol\ kN^{-1}\ s^{-1}$)
k_1	forward rate constant for nitric oxide oxidation (kPa^{-1})
K_{eq}	equilibrium constant for reaction Eq. (5)
K_H	heterogeneous equilibrium constant (kPa^{-2})
K_n	equilibrium constants for reactions tabulated in Table 1 ($n = 2$–5) ($kPa^{-2}\ s^{-1}$)
K_6	parameter defined by Eq. (2.22) ($kPa^{-1/2}$)
L	molar flow rate of water ($kmol\ s^{-1}$)
M_i	molecular weight of species i ($kg\ kmol^{-1}$)
N	number of catalyst screens
p_i	partial pressure of species i (kPa)
P	operating pressure (kPa)
$\boldsymbol{P}$	power (kW)
P_f	power factor
Q	flow rate ($m^3\ s^{-1}$)
r_{NH_3}	rate of mass transfer of ammonia on catalyst surface ($kmol\ m^{-3}\ s^{-1}$)
r_{PtO_2}	rate of platinum oxidation ($kmol\ m^{-3}\ s^{-1}$)
R	gas constant ($kJ\ kmol^{-1}\ K^{-1}$)
Ra_i	volumetric rates of mass transfer for species i ($kmol\ m^{-3}\ s^{-1}$)
Re	reynold's number
S	cross sectional area (m^2)
t	thickness (m)
T	temperature of operation (K)
u	fluid approach velocity ($m\ s^{-1}$)
V	volume (m^3)
w	weight percentage of nitric acid
x	conversion of ammonia to nitric oxide
X_N^*	moles of reactive nitrogen per mole of water
Y_i	moles of species i per mole of inert
$Y_{H_2O}^*$	moles of water per mole of inert
Y_N^*	moles of reactive nitrogen per mole of inert
Y_{NO}^*	moles of divalent nitrogen per mole of inert
z	length (m)

Greek letters

ΔP	pressure drop (kPa)
ε	volume fraction
ρ	density ($kg\ m^{-3}$)
τ	tortuosity factor

Subscripts

G	gas phase
i	inlet
L	liquid phase
n	stage number
o	outlet
s	screen
S	side stream

Superscripts

b	heterogeneous equilibria value
o	bulk
s	surface

N_2O_4, and the extent of reduction increases with an increase in the nitric acid concentration and finally approaching the equilibrium value. (iii) Substantial quantity of nitric acid is formed in the gas phase, at high temperature and pressure. (iv) The heat effects due to absorption and oxidation. (v) 1/3 mole of NO desorbs for every mole of NOx absorbed. This shows that the rate of oxidation and absorption/desorption are linked. (vi) Absorption rate of NO is negligible, however in the presence of NO_2, the NO forms N_2O_3 and subsequently HNO_2 because of the presence of H_2O vapor in the gas phase. The rates of N_2O_3 and HNO_2 absorption are very high as compared with even NO_2. Therefore the presence of NO_2 enhances the rate of absorption of NO. (vii) Maximum permissible concentration of nitric acid decreases with an increase in the mole fraction of nitric oxide. As the absorption continues, mole fraction of NO increases due to the absorption of N_2O_4, N_2O_3 and HNO_3. Therefore, multistage absorption is needed to get the desired concentration of nitric acid where, each stage comprises of an absorption section and an oxidation section. The plate spacing depends upon the gas phase composition and the desired extent of oxidation, also the extent of absorption on a stage is a variable. (viii) The effect of temperature is multifold. The rate of NO oxidation decreases whereas the rate of absorption increases with an increase in temperature. The equilibria (for the formation of N_2O_4 and N_2O_3) are favored at low temperature. Moreover, for a given NOx composition in the gas space, the maximum permissible nitric acid concentration increases with fall in temperature. (ix) Total pressure influences both the rates: NO oxidation and the NOx absorption.

In addition to the process of NOx absorption, ammonia oxidation and platinum losses from the catalyst screens also play a major role in optimization process. The heat recovery and power recovery are important aspects that need attention while developing a strategy for optimizing the process parameters for nitric acid process. The objective of the present work is to provide a strategy for improvement of production capacity and product quality in an operating plant, along with proposing an optimization strategy. The need was felt to develop models for all the units

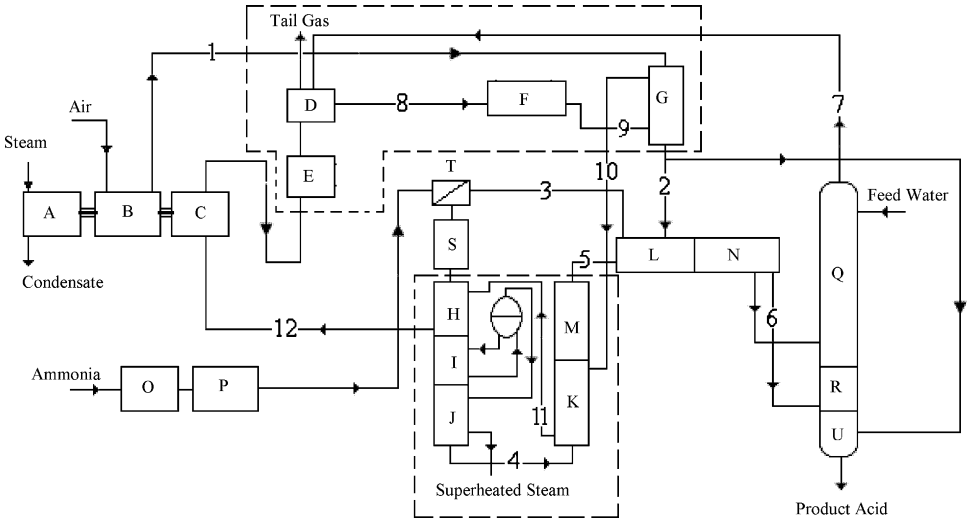

Fig. 1. Process flow diagram (PFD) (A: steam turbine, B: compressor, C: expander, D–L: heat exchanger, M: platinum filter, N: cooler/condenser, O: ammonia vaporizer, P: ammonia super heater, Q: absorber, R: oxidizer, S: reactor, T: static mixer, U: bleacher).

in the plant as they are interrelated and the operating parameters are strongly interacting.

2. Mathematical model

In order to develop an optimization strategy, it is important to identify various process parameters that influence the cost of operation. The costing models consider pressure drops across various equipment, compressor power requirement, pumping power requirement for cooling water in condenser and absorber, raw material requirements, catalyst requirements, associated process water requirement and the power for refrigeration. The mathematical models for practically all the equipment (which decide the capital and operating costs) have been described below. The reactions that are considered while developing these models are listed in Table 1, along with the various rate constants, equilibrium constants and heats of reaction/formation.

2.1. Ammonia oxidation reactor

Catalytic oxidation of ammonia is commercially one of the most important reactions in heterogeneous catalysis. Oele [12] has shown that the overall oxidation rate is controlled by the transfer of NH_3 from the bulk gas phase to the platinum surface. This claim has been verified, with respect to, the rate of chemical reaction model proposed by Fila and Bernauer [13]. In the range of parameters covered in this work (as presented in Table 2), it can be seen from Table 3, ammonia oxidation is

Table 1
Reactions considered in model development

Reactions	Equilibrium and rate constants	Standard heat of reaction (25 °C, kJ × 10^{-3})
(A) Gas phase		
$4NH_3+5O_2 \rightarrow 4NO+6H_2O$	N.A.	$H_1 = -226.60$ per kmol NH_3 oxidized
$2NO + O_2 \xrightarrow{k_1} 2NO_2$	$\log_{10} k_1 = (652.10/T) - 4.7470$	$H_2 = -57.11$ per kmol NO oxidized
$2NO_2 \overset{K_2}{\rightleftharpoons} N_2O_4$	$\log_{10} K_2 = (2993/T) - 11.2320$	$H_3 = -57.32$ per kmol N_2O_4 formed
$NO + NO_2 \overset{K_3}{\rightleftharpoons} N_2O_3$	$\log_{10} K_3 = (2072/T) - 9.2397$	$H_4 = -39.98$ per kmol N_2O_3 formed
$NO + NO_2 + H_2O \overset{K_4}{\rightleftharpoons} 2HNO_2$	$\log_{10} K_4 = (2051.17/T) - 8.7385$	$H_5 = -17.71$ per kmol HNO_3 formed
$3NO_2 + H_2O \overset{K_5}{\rightleftharpoons} 2HNO_3 + NO$	$\log_{10} K_5 = (2003.80/T) - 10.7630$	$H_6 = -20.53$ per kmol HNO_2 formed
Reactions		Standard heat of reaction (25 °C, kJ × 10^{-3})
(B) Liquid phase		
$2NO_2(g) + H_2O(l) \rightarrow HNO_3(l) + HNO_2(l)$		$H_7 = -53.68$ per kmol NO_2 absorbed
$N_2O_4(g) + H_2O(l) \rightarrow HNO_3(l) + HNO_2(l)$		$H_8 = -50.41$ per kmol N_2O_4 absorbed
$N_2O_3(g) + H_2O(l) \rightarrow 2HNO_2(l)$		$H_9 = -39.98$ per kmol N_2O_3 absorbed
$3HNO_2(l) \rightarrow HNO_3(l) + 2NO(g) + H_2O(l)$		$H_{10} = +23.90$ per kmol HNO_2 absorbed
$HNO_3(g) \rightarrow HNO_3(l)$		$H_{11} = -39.19$ per kmol HNO_3 absorbed
$HNO_2(g) \rightarrow HNO_2(l)$		$H_{12} = -41.45$ per kmol HNO_2 absorbed

Table 2
Process parameters used for model validations

	Units	Case 1	Case 2	Case 3
Production				
HNO_3 as 100% basis	TPD	300	300	300
Concentration of product acid	%	60.00	59.63	60.03
Compressor discharge pressure	kPa	1183	1295	1241
Reactor				
Ammonia selectivity to nitric oxide	%		90.0	
Cooler condenser				
Condensate temperature	°C	35	41	33
Condensate concentration	%	50	49.16	49.63
Absorption column				
Stages	–		38	
Diameter	m		3.2	
Absorption temperature	°C		40	
Chiller zone temperature	°C		20	

mass transfer controlled. This means that the value of ammonia partial pressure at the catalyst surface is zero. The overall rate is given by the following equation:

$$r_{NH_3} = k_G \underline{a}\, C_{NH_3} \tag{1}$$

Assuming the gas phase to be back mixed the number of catalyst screens is given as:

$$N = \frac{F_{i,NH_3} x}{k_G C_{NH_3} \hat{a} S} \quad \text{where} \quad \underline{a} = \hat{a} N S \tag{2}$$

The mass transfer coefficient for woven wire screen catalyst [14], surface area per unit volume of screens, the equivalent pore diameter (0.24 mm) and the voidage (0.81) were evaluated using the procedures given by Armour and Cannon [15]. The pressure drop across the screen was estimated using the following equation:

$$\Delta P = \frac{f \tau t \rho u^2}{\varepsilon_s^2 D} \tag{3}$$

where the friction factor for the screen is given by [15]:

$$f = \frac{8.61}{Re} + 0.52 \tag{4}$$

In order to carry out the optimization exercise, it is imperative to evaluate the platinum losses occurring under various operating conditions in the plant. It has been known [16] that the observed volatility of the platinum group metals in the presence of oxygen is higher than that for pure metal and the enhanced volatility has been attributed to the formation of volatile oxides. At temperatures above approximately 1073 K, platinum oxidizes slowly to produce a volatile species PtO_2 [17]. Also it has been shown [18] that the losses due to mechanical attrition are negligible.

During the catalytic oxidation of ammonia, X-ray microanalysis [19] has shown that the rhodium oxide also gets formed on the surface of the Pt-Rh gauzes. The oxidation of platinum is a reversible reaction. However, the product PtO_2 is transferred to the gas phase which favors the forward reaction:

$$Pt + O_2 \underset{k_b}{\overset{k_f}{\rightleftharpoons}} PtO_2 \tag{5}$$

Mass transfer coefficients [14] (for PtO_2) have been calculated for specific geometries [15] and flow conditions of the catalyst screens. The equilibrium constant has been evaluated from the experimental data of Alock and Hooper [17]. The overall rate of mass transfer accompanied by the chemical reaction has been derived by Bartlett [20]. The platinum losses due to PtO_2 formation can be given as [20]:

$$r_{PtO_2} = \frac{k_G \underline{a} (2\pi M_{PtO_2} RT)^{-1/2} K_{eq} C_{O_2}}{\{k_G/RT + (2\pi M_{PtO_2} RT)^{-1/2}\}} \tag{6}$$

Table 3
Comparison of mass transfer and chemical reaction rates for ammonia oxidation

Parameter	Rate of ammonia oxidation (kmol/m^2 s)		% Increase of chemical reaction rate to mass transfer rate
	Mass transfer controlling [12]	Chemical reaction controlling [13]	
Pressure (kPa)			
900	1.25e-3	1.72e-3	37.60
1100	1.25e-3	1.92e-3	53.60
1300	1.25e-3	2.08e-3	66.40
1500	1.25e-3	2.24e-3	79.20
1700	1.25e-3	2.38e-3	90.40
Inlet temperature of ammonia oxidation reactor (°C)			
210	1.25e-3	2.04e-3	63.20
230	1.25e-3	2.08e-3	66.40
250	1.25e-3	2.12e-3	69.60
270	1.25e-3	2.16e-3	72.80
Excess air to ammonia oxidation reactor (wt%)			
7	1.27e-3	2.14e-3	69.17
9	1.26e-3	2.11e-3	67.46
11	1.25e-3	2.08e-3	66.40
13	1.24e-3	2.06e-3	64.80

Parameters considered for rate comparison (otherwise mentioned): capacity = 300 TPD (100% HNO_3 basis); quality of acid = 60 wt% (HNO_3); inlet temperature to ammonia oxidation reactor = 230 °C; excess air = 11 wt%; operating pressure = 1300 kPa; selectivity of ammonia to nitric oxide = 90%.

2.2. Heat exchanger network

The gases leave the ammonia reactor/oxidizer at about 1173 K whereas the NO*x* absorber operates in the range of 328–318 K. Therefore, the gases need to be cooled in such a way that the enthalpy is used advantageously for steam generation and for preheating various streams. These features need to be included in the heat exchanger network which contributes to the capital cost as well as operating cost due to pressure drop. The present model for heat exchanger network, addresses to all these aspects along with the chemical reaction taking place within the exchangers.

The model uses appropriate methods for the estimation of pressure drop across the tube bank [21] which includes due consideration of the geometric layout for the tube banks [22]. The contribution to shell side pressure drop by, cross flow, baffle windows and end zones have been considered. The shell side heat transfer coefficient was corrected for segmental baffle window, baffle leakage, bypass, non equal inlet-outlet baffle spacing, etc. The shell side corrections over an ideal shell side pressure drop

and heat transfer coefficient were estimated according to the recommendations of Bell-Delaware [23].

The chemical reactions occurring in the heat exchanger train were considered according to the model presented later in the section on the oxidizer. Plug flow behavior was considered in the tubes of the heat exchanger, as the peclet number was found to be greater than 30. Details on mass balance, heat balance, gas equilibria and method of solution of the model equations have been given in Appendix A.

2.3. Condenser

Condensers are generally large surface area heat exchangers. The process gas enters from the preceding heat exchanger which contains NO*x* gases, N_2, unreacted O_2 and water vapor as a product of ammonia oxidation reaction. In the process design of nitric acid plant, the design of condenser is crucial for obtaining the desired concentration of product acid from the absorption section. A number of chemical reactions and chemico-physical phenomena; like (i) nitric oxide oxidation, (ii) formation of higher nitrogen oxides, (iii) water condensation, and (iv) absorption of nitrogen oxides; occur in condenser. The present model accounts for gas-phase reactions and equilibria, condensation, and the effect of heterogeneous equilibria on the condensate concentration. The model considers water entering the condenser in the form of vapor, majority of which condenses and then reacts to form nitric and nitrous acid in the liquid phase.

The methodology for solving the material balance of the condenser is as follows: (i) concentration of nitric acid in condensate is assumed, (ii) the nitrogen mole fraction at the inlet is above 0.85. The outlet mole fraction is assumed which permits the estimation of total molar gas flow rate at the condenser exit (iii) from the nitric acid concentration and temperature of the condensate, the partial pressure of nitric acid and water in the gas phase were evaluated and which, in turn, enabled the estimation of the amount of water condensed, (iv) the oxidation of NO to NO_2 in the condenser tubes was calculated using the models described in Appendix A, (v) the reactive nitrogen in the outlet gas was estimated from the difference of the reactive nitrogen at the inlet (to condenser) and the reactive nitrogen in the condensate, (vi) the individual composition of NO*x* gases at the condenser was estimated from the gas phase equilibria described in Appendix A, (vii) with known quantities of NO and N_2O_4, the equilibrium concentration of nitric acid leaving the condenser was evaluated using the procedure of Carberry [11], (viii) the HNO_3 concentration obtained in step (vii) was replaced by the assumed concentration in the step (i) and all the steps were repeated for convergence so as to achieve complete balances at the elemental level on nitrogen, reactive nitrogen, hydrogen and oxygen, (viii) finally heat balance and pressure drop were estimated across the condenser.

2.4. Oxidizer or preconditioning zone

The NO*x* gases leaving the heat exchanger train contains mainly nitric oxide and needs further oxidation prior to absorption. The oxidizer is usually a part of the absorption column and occupies the volume beneath the bottom-most tray. The heterogeneous equilibrium between NO (g) and HNO_3 (l) controls the nitric acid concentration for a given partial pressure of NO*x* gases. Therefore the oxidizer is important equipment for the manufacture of nitric acid with high concentration.

A differential mass balance for the NO oxidation is given by:

$$\frac{dY^*_{NO}}{dz} = -\frac{S}{G}[k_1(p_{NO})^2 p_{O_2}] \quad (7)$$

The oxygen balance is given by:

$$\frac{dY^*_{O_2}}{dz} = -\frac{1}{2} \times \frac{S}{G}[k_1(p_{NO})^2 p_{O_2}] \quad (8)$$

In addition to the formation of the nitrogen dioxide, other nitrogen oxides (N_2O_3 and N_2O_4) and oxyacids are formed according to the equilibria described in Table 1(A). Further, the heat balance effects of these reactions result into a temperature profile along the length of oxidizer. The method of solution of material balance across the oxidizer along with the heat balance is given in Appendix A.

2.5. Absorption column

The literature shows the development phases which started with the graphical method [24] which involved a modified McCabe-Thiele method, considering only NO, NO_2 and N_2O_4 in the gas phase, the models thereafter developed accounted for (i) extensive heat balance [25], (ii) gas phase equilibria [26,27] and the gas phase oxidation of NO to NO_2, (iii) formation [28] of HNO_2 and HNO_3, (iv) simultaneous absorption of NO_2, N_2O_3 and N_2O_4 with chemical reaction [29] with water and the dependence of these rates on nitric acid concentration and temperature, (v) heterogeneous gas–liquid equilibria [30], (vi) HNO_2 decomposition [26] in the liquid phase, (vii) desorption of NO preceded by chemical reaction [30]. The effect of low solubility of NO and the back pressure due to heterogeneous equilibria neglected previously [31,32] have been accounted in the model developed in this work.

The increasingly stringent environmental protection regulations, has made it necessary to develop optimization strategies for keeping the NO*x* emissions within permissible limits.

2.5.1. Absorption stage on a plate

In the present work a plate column having bubble cap trays has been considered. The following assumptions have been made (i) the liquid phase is completely back-mixed on a plate and the gas phase moves in a plug flow manner, (ii) liquid hold up is uniform throughout the plate, (iii) the gas follows an ideal behavior, (iv) column operates under steady state.

The component balances for the gas and liquid phases are described in Appendix B. The overall material balance for an absorption stage is given by the following equations:

Reactive nitrogen:

$$G(Y^*_{N,n-1} - Y^*_{N,n}) = L_n X^*_{N,n} - L_{n+1} X^*_{N,n+1} - L_S X^*_{N,S} \quad (9)$$

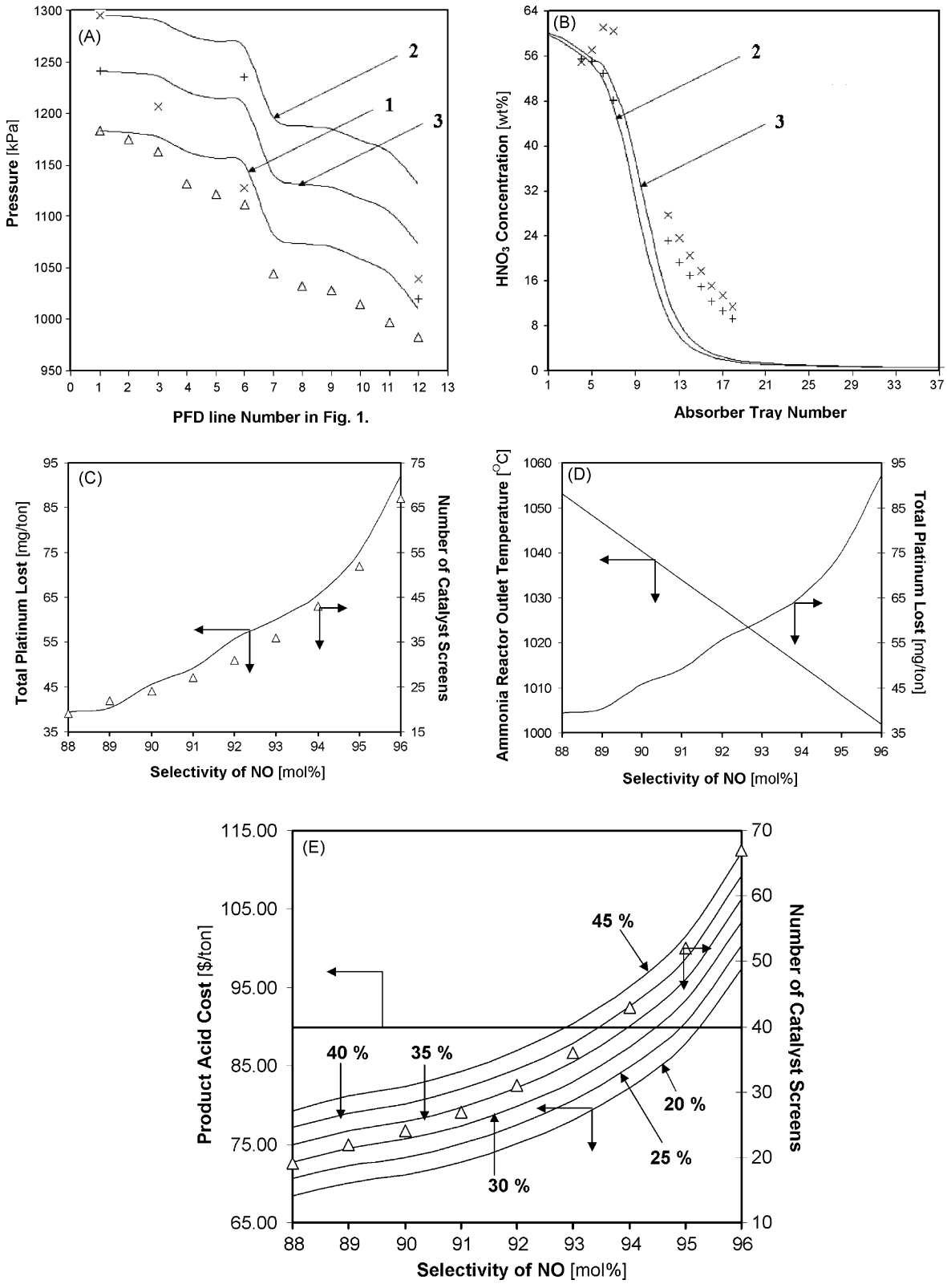

Fig. 2. Profiles for a 300 TPD plant with 60% weight product quality for different cases as presented in Table 1: (A) pressure profile in plant at various locations. (B) Nitric acid concentration profile on trays. Case 1: (Δ) reported, (—) simulated. Case 2: (×) reported, (—) simulated. Case 3: (+) reported (—) simulated. (C) Catalyst screen requirement and platinum losses for various NO selectivity. (D) Reactor outlet temperature and platinum losses for various NO selectivity. (E) Cost of product acid and catalyst screen requirement for various NO selectivity.

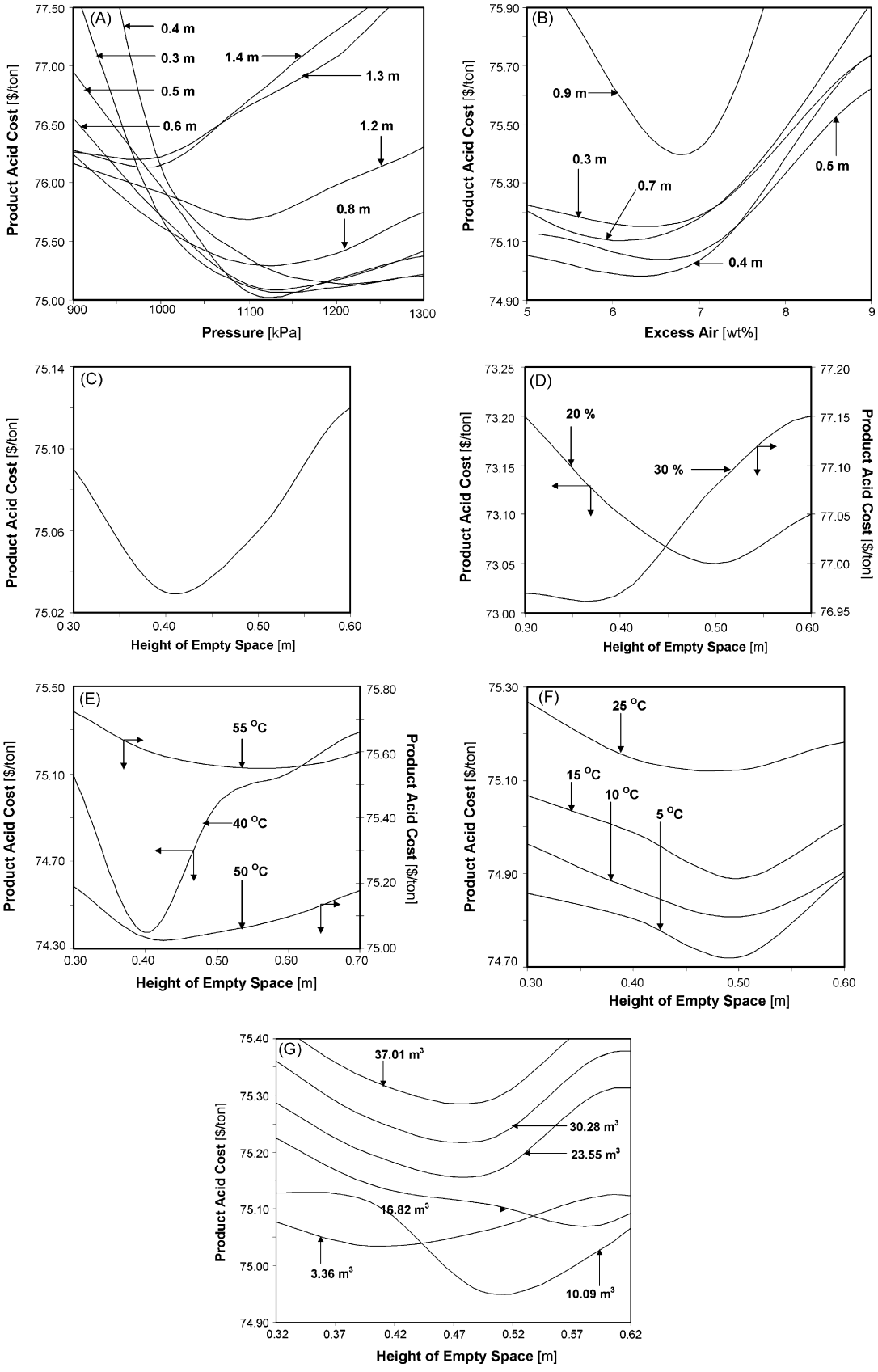

Fig. 3. (A) Optimum pressure and gas space height at 3% (wt) excess air. (B) Optimum excess air and gas space height at 1125 kPa total pressure. (C) Optimum gas space height for a wide range of excess air (3–15% (wt)) and total pressure (900–1700 kPa). (D) Effect of fixed capital contribution on optimum gas space height. (E) Effect of absorber tray temperature on optimum gas space height. (F) Effect of chiller zone temperature on optimum gas space height. (G) Effect of oxidizer volume on optimum gas space height.

Water and water vapor:

$$G(Y^*_{H_2O,n-1} - Y^*_{H_2O,n}) = L_n\left(\frac{1+X^*_{N,n}}{2}\right) - L_{n+1}\left(\frac{1+X^*_{N,n+1}}{2}\right) - L_S \times \left(\frac{1+X^*_{N,S}}{2}\right) \quad (10)$$

2.5.2. Empty section or space between plates

The empty section or the space between plates acts as an oxidizer for NO and the oxidizer model has been given in Appendix A. The rise in temperature in empty section was based on the heat balance. The empty section plays an important role as it decides the relative proportion of tetravalent to divalent nitrogen oxides entering the next plate and hence it also decides the maximum permissible concentration of HNO_3 leaving the plate.

2.5.3. Estimation of design parameters

The design parameters such as fractional liquid hold up, fractional gas hold up, gas and liquid side mass transfer coefficients [33], dry tray and wet tray pressure drops for the bubble cap trays were estimated according to the procedures of Bolle and Dauphine [34].

2.5.4. Heat balance

The heat balance for the above two parts were modeled separately. In absorption on a stage, the heat balance is accounted for gas and liquid phase as: (i) rate of formation of N_2O_3 from NO and NO_2, (ii) rate of formation of N_2O_4 from NO_2, (iii) rate of formation of HNO_3, (iv) rate of formation of HNO_2, (v) rate of heat liberated due to oxidation of NO, and (vi) rate of water evaporation. In the empty section, heat balance was modeled as outlined for oxidizer. The values of heats of various reactions have been given in Table 1.

2.6. Compressor and expander

For the estimation of compressor power an isothermal condition has been assumed (as the compression heat is removed during the stages) and is given by:

$$\boldsymbol{P} = P_i Q \ln\left(\frac{P_o/P_i}{eP_f}\right) \quad (11)$$

Compressor efficiency and power factor have been taken as 65% and 75%, respectively.

The high pressure low temperature gases emitted at the exit of absorption column, are heated and passed through the expander for power recovery. A certain percentage of the power recovery (70%) was incorporated in the cost calculations.

2.7. Pump

The process water required for the absorption and the cooling water required on trays are pumped to their respective locations. The pumping power requirement for the process water was estimated based on the height of absorption column:

$$\boldsymbol{P} = \frac{H\rho g Q}{e} \quad (12)$$

For the estimation of power for cooling water, the pressure drops in the water line were suitably calculated.

3. Results and discussion

The models developed in this work are aimed at providing a strategy for optimization of the capacity and/or the HNO_3 product concentration. The cost calculations are presented for per ton of product acid. The components of fixed cost include: (i) reactor/catalyst, (ii) heat exchangers, (iii) oxidizer, (iv) absorption column, and (v) compressor or expander. The fixed cost was annualized at 25% towards depreciation, interest, maintenance, etc. The operating cost includes (i) ammonia consumption, (ii) power required for compressor, (iii) chiller load, (iv) power for pumping, (v) catalyst loss, (vi) process water, and (vii) cooling water requirements. The power is recovered in the plant by the expander and the steam turbine. Additional operating expenses like, overheads, insurance, etc. were also included in the overall cost calculations.

A typical weightage of various parameters contributing to total cost of production per ton of product acid is as follows: ammonia 45%, power 29.5%, water 2.2%, chiller 1%, catalyst replacement 7%, column 5.5%, heat exchanger 4%, catalyst 0.8%, and additional costs 5% which mainly includes overheads. It may be noted that the first five parameters are of recurring type whereas the next three are of capital in nature and have been suitably annualized.

Table 4
Plant simulation results

Process parameter	Unit (per ton 100% HNO_3)	Reported value	Simulated value
Reactor			
Conversion in NH_3 reactor	–	90	90
Number of screens in NH_3 reactor	–	28	24
Platinum losses in NH_3 reactor	mg	–	40.24
Waste heat boiler			
Steam generation	tonnes	14.4	12.81
Condenser			
Heat duty	kW	487	313
Reactive nitrogen in gas outlet	kmol h^{-1}	107	106
Reactive nitrogen in liquid outlet	kmol h^{-1}	87	91
HNO_3 concentration in condensate	wt%	50.12	49.75
Absorber			
Cooling water	m^3 h^{-1}	637	537
Power			
Compressor power (consumption)	kW h	6527	7165
Expander power (generation)	kW h	5421	5363

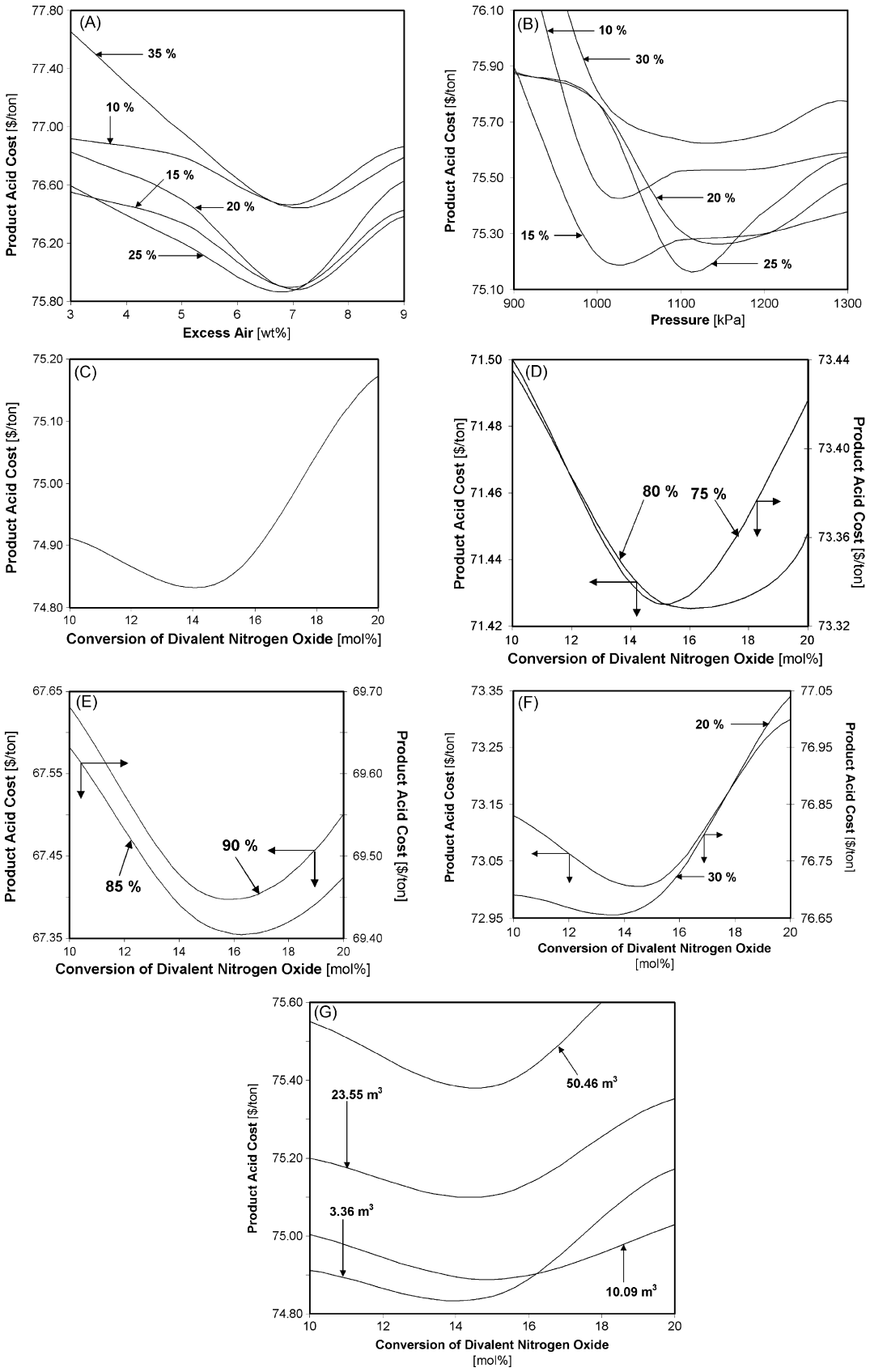

Fig. 4. (A) Optimum excess air and equal divalent nitrogen conversion at 900 kPa total pressure. (B) Optimum pressure and equal divalent nitrogen conversion at 6.8% (wt) excess air. (C) Optimum divalent nitrogen conversion for a wide range of excess air (3–15% (wt)) and total pressure (900–1700 kPa). (D) Effect of 75% and 80% power recovery on optimum divalent nitrogen conversion. (E) Effect of 85% and 90% power recovery on optimum divalent nitrogen conversion. (F) Effect of fixed capital contribution on optimum divalent nitrogen conversion. (G) Effect of oxidizer volume on optimum divalent nitrogen conversion.

3.1. Plant simulation

Table 2 presents the process parameters of an operating plant used for the model validation. The pressure profile predicted by simulation is compared with the plant data in Fig. 2A. A good agreement (within 3.5%) can be observed between the model predictions and the plant data. The comparison of model predictions for the HNO_3 concentration with the plant data is presented in Fig. 2B. These predictions are also in good agreement with the plant data, within ±5%. The other parameters obtained from the simulations have been compared with the plant data in Table 4, which shows an agreement within ±10 to 15%. The effect of NO selectivity on platinum losses is depicted in Fig. 2C and Fig. 2D. It can be observed that the reactor outlet temperature drops with an increase in the NO selectivity. This observation has main effect on the catalyst screen requirement which increases with an increase in the extent of NH_3 requirement for desired NO selectivity. Fig. 2E shows, the effect of percentage fixed capital contribution to annualized product acid cost for various NO selectivity. It has been observed that, for a 300 TPD (100% basis of HNO_3) and 60% product quality, NO selectivity above 92% makes the annualized catalyst cost to be prohibitively high.

3.2. Strategy for optimization

Process parameters like pressure, excess air, absorber tray temperature and chiller zone temperature have a profound effect on the cost of production. Hence, it was thought desirable to develop an optimization strategy for designing a nitric acid plant with a capacity of 300 TPD (100% HNO_3 basis) and 60% product quality. For this purpose the outlet NO*x* has been considered at 200 ppmV. Two strategies adopted for the optimum design of absorber have been discussed below:

3.2.1. Absorber with equi-spaced plates

The empty space (here in after, termed as gas space) in every stage was considered to possess the same volume throughout the length of the absorber, in this discussion.

Fig. 3A shows that the operating pressure plays a dominant role on the gas space volume. Low height increases the fixed capital contribution as more number of stages is required to achieve the desired outlet NO*x* of 200 ppmV. As the height of the gas space increases, the conversion of divalent to tetravalent nitrogen oxide increases, which in turn, increases the absorption efficiency thereby, reducing the number of stages. Further, increase pressure increases the operating cost and decreases the

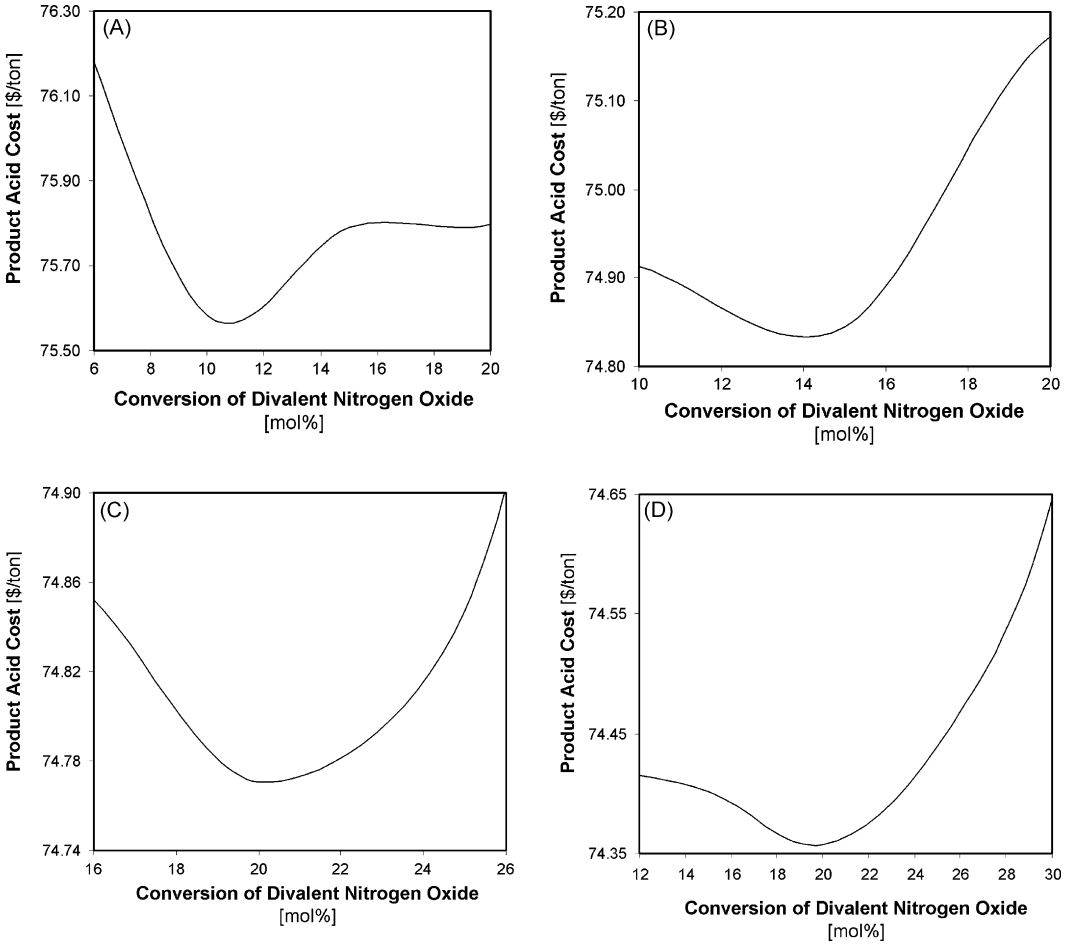

Fig. 5. Effect of outlet NO*x* (ppmV) on optimum divalent nitrogen conversion: (A) 150, (B) 200, (C) 250, (D) 300.

capital cost because of the lower number of stage requirement. A comprehensive parametric sensitivity analysis has shown that for the case of 3% (wt) excess air, the optimum height of gas space is 0.50 m, the operating pressure is 1125 kPa, and this results into the product acid cost to be 75.05 $/ton.

Fig. 3B shows that the optimum excess air was 6.5% (wt) and optimum height of empty space was 0.40 m, for an operating pressure of 1125 kPa. Increasing the percent excess air, increases the partial pressure of oxygen, leading to enhanced oxidation; thus reducing the number of stages required to achieve the constrain of 200 ppmV NO*x* at the absorber outlet. The total cost in this case works out to be 75.00 $/ton.

In addition to the above two results, simulations were performed over a wide range of excess air (3–15% (wt)) and total pressure (900–1700 kPa). The results are shown in Fig. 3C. For 7% (wt) excess air, the optimum height was found to be 0.42 m and the optimum pressure to be 1100 kPa, respectively. For this case the capital cost was annualized at the rate of 25%. However, if we take 20% as the basis, the optimum gas space height was found to be 0.5 m whereas for 30% case, the optimum height was 0.38 m, as shown in Fig. 3D. Therefore, for a 50% variation in the fixed cost contribution, the variation in the optimum height of gas space works out to be 30% and the variation in the total product acid cost is 5%.

The temperature plays a pivot role in the equilibria of gas phase reactions, thereby, influencing the composition of NO*x* gases. The equilibrium constant correlations provided in Table 1A shows that the gas phase equilibria are favored by low temperature operation. Fig. 3E shows the effect of absorber tray temperature for an operating pressure of 1125 kPa on the optimum gas space height. For a temperature of 40 °C the value was 0.40 m and the excess air was 7% (wt). Similarly, for 50 °C the optimum gas space height was 0.42 m and the excess air was 7% (wt). Also, for 55 °C the optimum gas space height was 0.52 m and the excess air was 5% (wt). For a 10 °C raise from 40 °C to 50 °C, the height increased by 5%; however, a 5 °C raise from 50 °C to 55 °C showed an increase by 25%. It is therefore recommended to operate the absorber at tray temperatures below 50 °C which is retainable easily obtainable by the cooling water from cooling towers.

Fig. 3F shows the effect of chiller zone temperature on the optimum gas space height at an operating pressure of 1125 kPa. For a temperature range of 5–15 °C, the optimum height was 0.50 m, however, when operated at 20 °C the optimum height was 0.42 m. The reduction of temperature increases the rate of NO oxidation and hence reduces the empty space height. The fixed capital contributing to the annualized product cost thereby reduces and compensates for the higher chiller operating cost

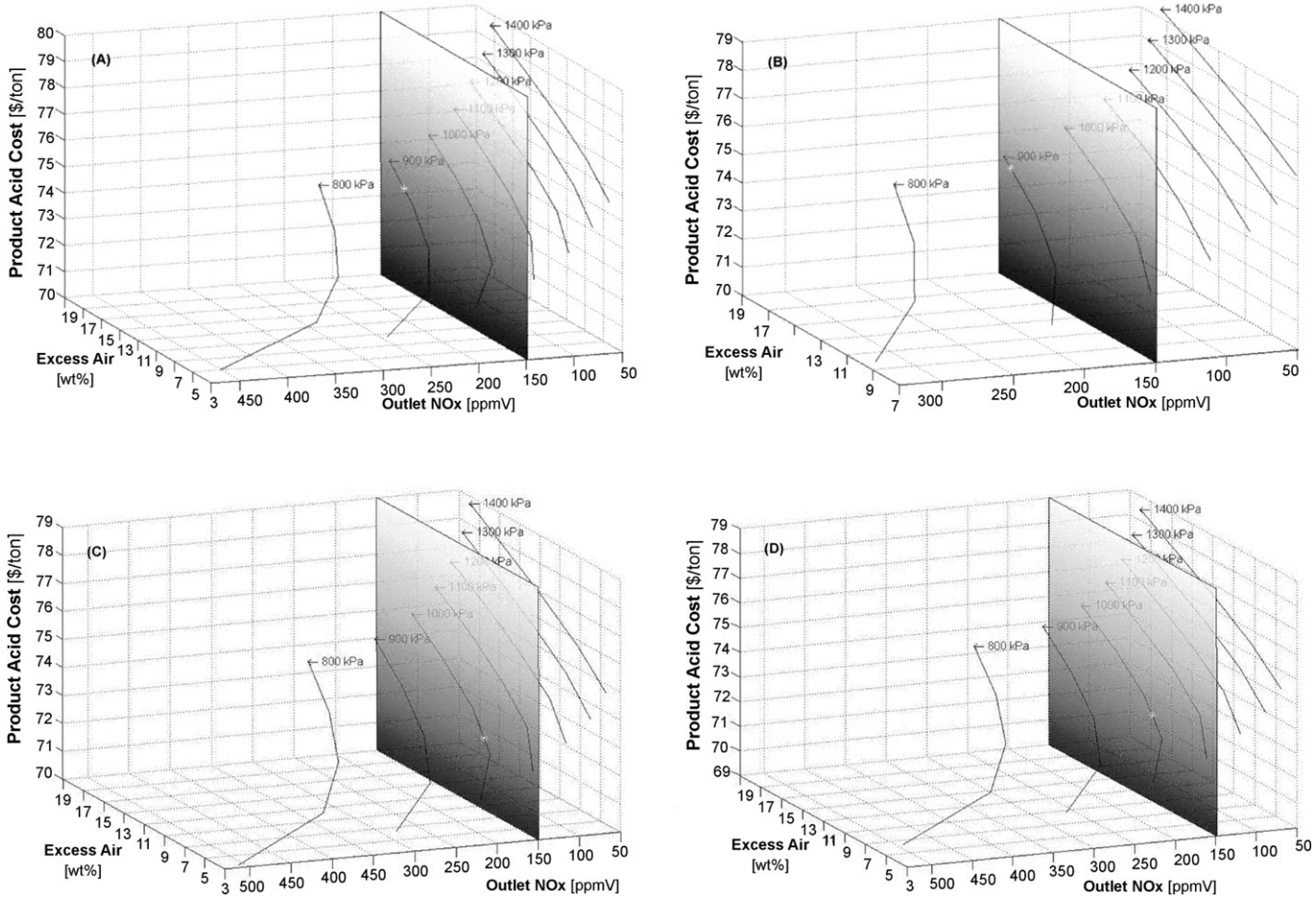

Fig. 6. Optimum operating conditions under constrain of 150 ppmV NO*x* at outlet (60% product quality). Effect of pressure and excess air for: (A) 300 TPD, (B) 310 TPD, (C) 320 TPD, (D) 330 TPD.

at reduced temperatures. At 20 °C, to meet the constrain of absorber outlet NO*x*, more stages were required, the decrease in chiller cost here was compensated by high fixed capital contributed by increased stages, giving an optimum at reduced gas space height of 0.42 m.

Fig. 3G shows the effect of oxidizer volume on the product acid cost. The importance of the role of oxidizer has been explained earlier. Higher concentration of tetravalent nitrogen oxides enhances the overall rate of absorption. This effect can be clearly realized from Fig. 3G. Higher oxidation volume helps in reducing the number of stages required for achieving a desired constraint of NO*x*. As the oxidizer volume is increased to about 3 times the original volume (i.e. 3.67 m^3) that is 10.09 m^3, the optimum results work out to be 0.51 m for gas space height, 1100 kPa operating pressure and 7% (wt) for excess air.

3.2.2. Absorber with equal conversion of divalent nitrogen oxide in gas space

It was thought desirable to keep the same extent of conversion in all the empty spaces. Fig. 4A shows that for an operating pressure of 900 kPa, for a range of excess air (3–9% (wt)), the optimum divalent nitrogen conversion that can be selected for designing the absorber was 25%. The optimum excess air as can be observed was 6.80% (wt). However, simulation studies carried out for a pressure range of 900–1300 kPa for the 6.80% (wt) of excess air (Fig. 4B), gave an optimum conversion of 25% for an operating pressure of 1125 kPa. Hence, it was thought desirable to carry out the search for optimum divalent nitrogen conversion for operating conditions over a range of 900–1700 kPa pressure and 3–15% (wt) excess air. Fig. 4C shows that for a compressor power recovery of 70%, the optimum cost of product acid was 74.83 $/ton, for the conversion level of 14%, 1300 kPa pressure and 3% (wt) excess air.

The recovery of compressor power plays an essential role, as power contributes 29.50% to the annualized cost of product acid on the basis of 25% fixed capital contribution per year. Fig. 4D and E show that the optimum divalent nitrogen conversion was in the range of 14–16.20%, for a wide range of total pressure (900–1700 kPa) and excess air (3–15% (wt)), over a 30% variation in power recovery thus, suggesting the influence of power recovery on the change in optima to be negligible.

Studies from Fig. 3C and D and Fig. 4C–E suggest that designing the absorber by the method of equal conversion in gas space, helps to realize a lower cost of product acid as compared to the method of equi-spaced plates. By choosing the equal conversion method, the volume requirement for every stage needs to be estimated, thus providing a variable height of gas space for plate spacing to meet the constrain of NO*x* at outlet to absorber. How-

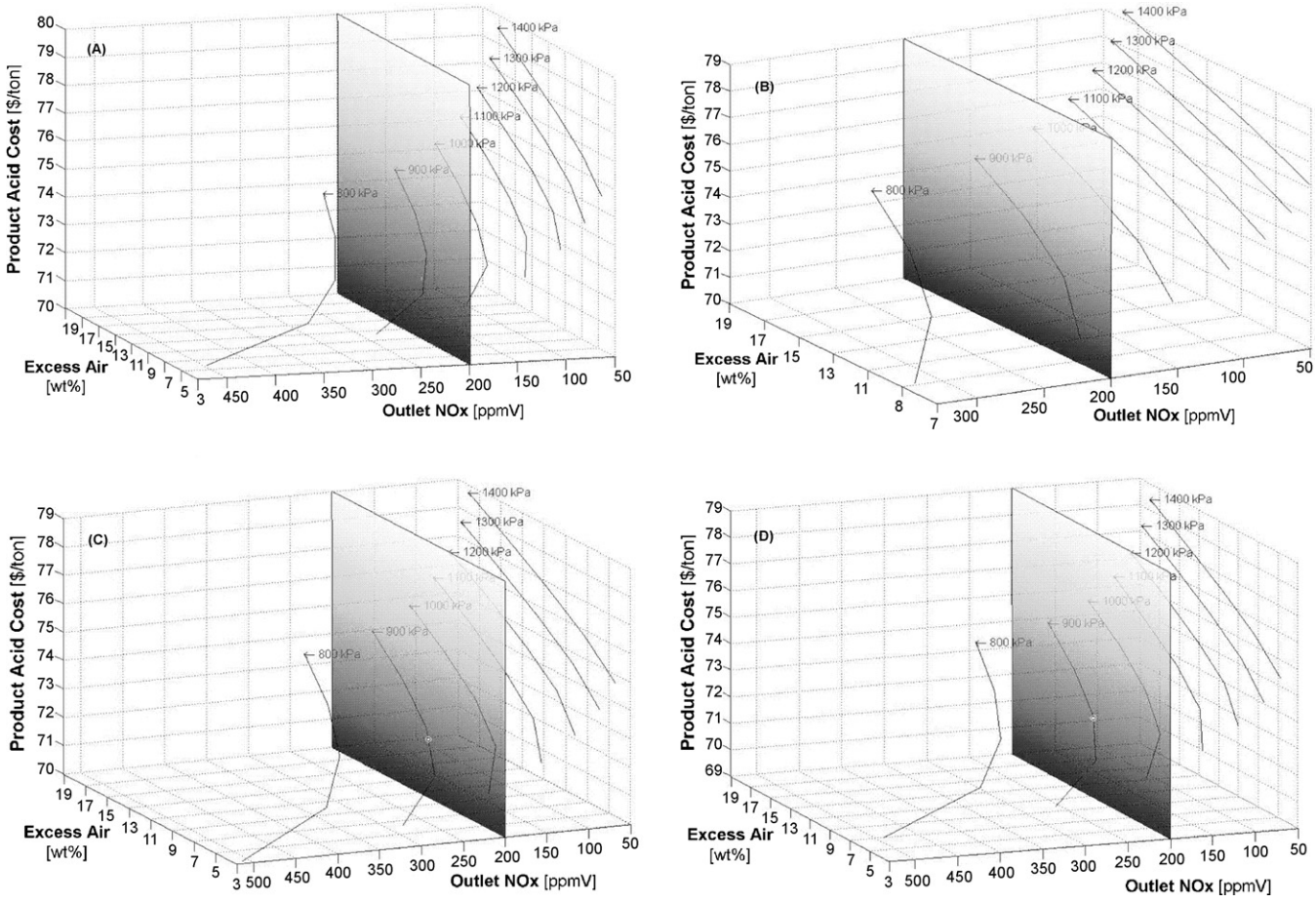

Fig. 7. Optimum operating conditions under constrain of 200 ppmV NO*x* at outlet (60% product quality). Effect of pressure and excess air for: (A) 300 TPD, (B) 310 TPD, (C) 320 TPD, (D) 330 TPD.

ever, by following the method of equi-spaced plates, it may be pointed out that the resulting constant volume does not provide optimum level of conversion which is needed for the absorption on the next plate with its corresponding HNO_3 concentration and temperature.

Keeping the above discussion in view, the sensitivity of the per cent annualized fixed capital was studied. It can be seen from Fig. 4C that the optimum levels of conversion, pressure and per cent excess air was 14%, 1300 kPa and 3% (wt), respectively. Further, in the range of 20–30% rate of annualization, as shown in Fig. 4F, the optimum conversion can be seen to be in the range of 15–13% respectively.

Fig. 4G shows the effect of oxidizer volume on the product acid cost. As against the earlier study for equi-spaced case of absorber; as the conversion of divalent nitrogen is considered equal in every stage, hence we get a variable volume of gas space along the length of the absorber. Thereby, the effect of volume variation on the performance of the column is not pronounced as shown in the figure.

Fig. 5A–D show that as the demand for outlet NO*x* constrain becomes stringent, the optimum cost for product acid increases and so does the process conditions. For 150 ppmV outlet NO*x* constrain the optimum levels of conversion, pressure and per cent (wt) excess air were found to be 11%, 1400 kPa and 3% (wt), respectively. So for 200, 250 and 300 ppmV the optimum divalent nitrogen conversion was 14%, 19% and 20%, respectively. The respective optimum values of other parameters were 1300 kPa pressure and 3% (wt) excess air, 1100 kPa pressure and 5% (wt) excess air; and 1100 kPa pressure and 3% (wt) excess air. Fig. 5 shows that, above 250 ppmV, the optimum divalent nitrogen oxide conversion practically remains constant (20%). Below this level of constraint from 250 ppmV to 100 ppmV, the optimum level of conversion was found to increase by 8%.

3.3. Strategy for capacity improvement

A 300 TPD (100% HNO_3 basis) plant, 60% by weight of product acid, was taken as a case study to assess the model to provide for the optimum operating conditions. The objective was, under otherwise identical conditions of the existing plant and the environmental constrain of ppmV NO*x* at the outlet, to seek the possibility of increasing the capacity and/or concentration of product HNO_3 (herein after termed as quality).

3.3.1. Effect of outlet NOx concentration

Fig. 6A–D show, as the production of the plant is increased, for an absorber tray temperature of 40 °C and chiller zone

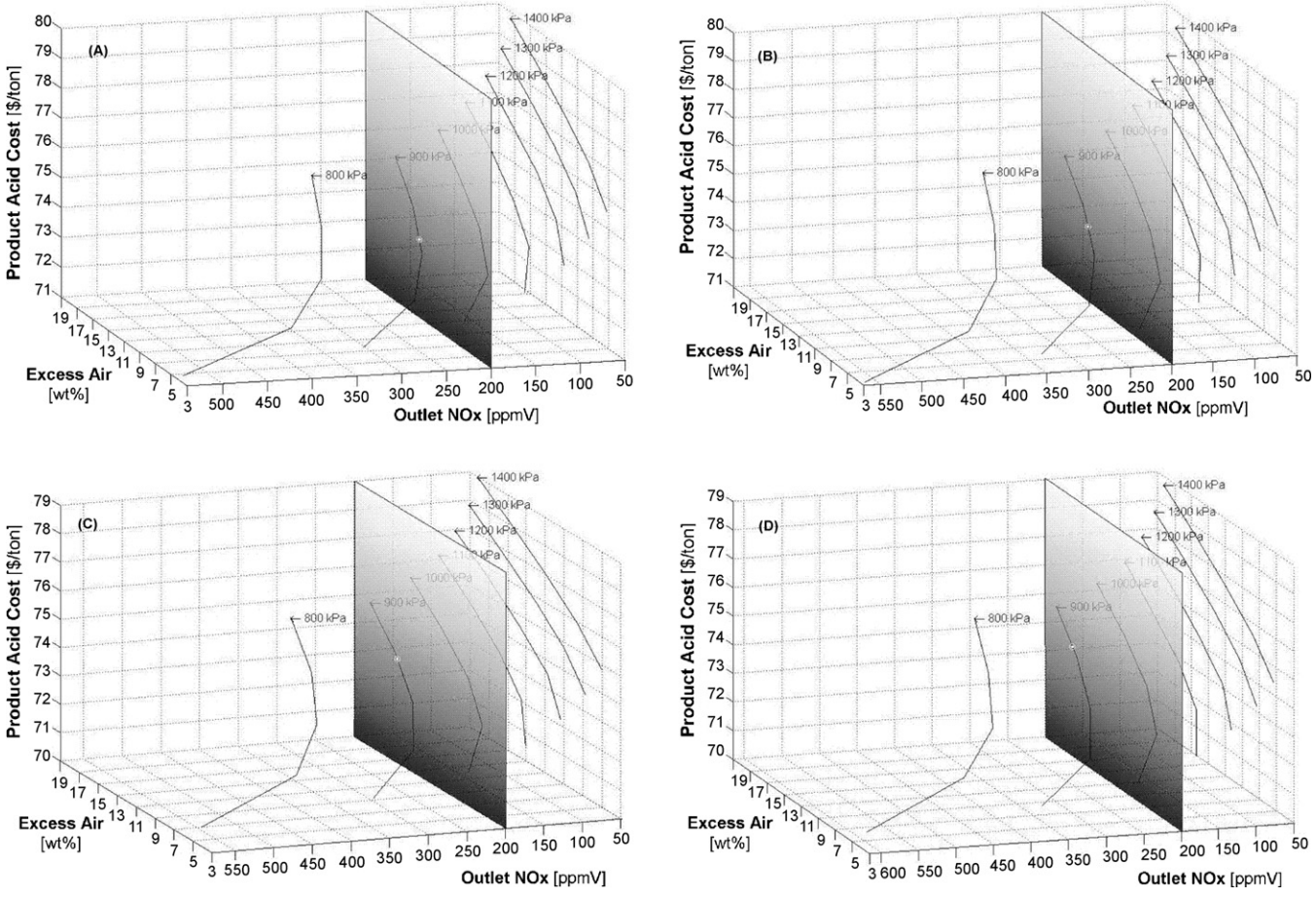

Fig. 8. Optimum operating conditions under constrain of 200 ppmV NO*x* at outlet (60% product quality). Effect of pressure and excess air; at absorber tray temperature of 50 °C for: (A) 300 TPD, (B) 310 TPD, (C) 320 TPD, (D) 330 TPD.

temperature of 10 °C, the production cost per ton of product acid reduces. Simulations have been carried out for a pressure range of 800–1400 kPa and excess air range of 3–19% (wt). The shaded plane in the figures is the 150 ppmV outlet NO*x* constrain, and the 3D view of the figures give the operating conditions meeting the constrain. The optimum observed for 300 TPD is 72.79 $/ton operating at 1000 kPa and 6.88% (wt) excess air; for 310 TPD is 72.65 $/ton operating at 1000 kPa and 7.60% (wt) excess air; for 320 TPD is 72.55 $/ton operating at 1000 kPa and 8.40% (wt) excess air; and for 330 TPD is 72.39 $/ton operating at 1100 kPa and 4.18% (wt) excess air. Therefore, a 10 TPD capacity increase, improves profit by 4.22% and for a 10% rise in capacity to 330 TPD, profit margin improves by 12.71%; i.e. 1031 $/day.

Fig. 7A–D show the optimum for constrain of 200 ppmV outlet NO*x*. The optimum for 300 TPD is 72.20 $/ton operating at 900 kPa and 8.54% (wt) excess air; for 310 TPD is 72.11 $/ton operating at 900 kPa and 9.34% (wt) excess air; for 320 TPD is 71.83 $/ton operating at 1000 kPa and 4.32% (wt) excess air; and for 330 TPD is 71.67 $/ton operating at 1000 kPa and 4.80% (wt) excess air. Therefore, for a 50 ppmV reduction in the NO*x* outlet constrain and a 10% rise in capacity to 330 TPD, improves profit margin by 13.47%; i.e. 1132 $/day.

3.3.2. Effect of absorber tray temperature

Fig. 8A–D show the effect of 10 °C rise in absorber tray temperature for various capacities on the cost of production. For, a chiller zone temperature of 10 °C, a constrain of 200 ppmV outlet NO*x* gives optimum for 300 TPD, as 72.96 $/ton operating at 1000 kPa and 4.98% (wt) excess air; for 310 TPD, as 72.75 $/ton operating at 1000 kPa and 5.46% (wt) excess air; for 320 TPD, as 72.58 $/ton operating at 1000 kPa and 5.91% (wt) excess air; and for 330 TPD, as 72.41 $/ton operating at 1000 kPa and 6.33% (wt) excess air. Therefore, if operated at 40 °C instead of 50 °C, reduction in operating cost by 1.1% per ton of product acid is possible; which translates into a profit enhancement of 4.74% for 300 TPD plant. Also, when capacity is increased by 10%, a reduction in operating cost by 1.8% per ton of product acid, is possible; which translates into a profit enhancement by 18.84% or 1511 $/day.

3.3.3. Effect of chiller zone temperature

Fig. 9A–D show, the effect of 10 °C rise in chiller zone temperature for various capacities on the cost of production. For

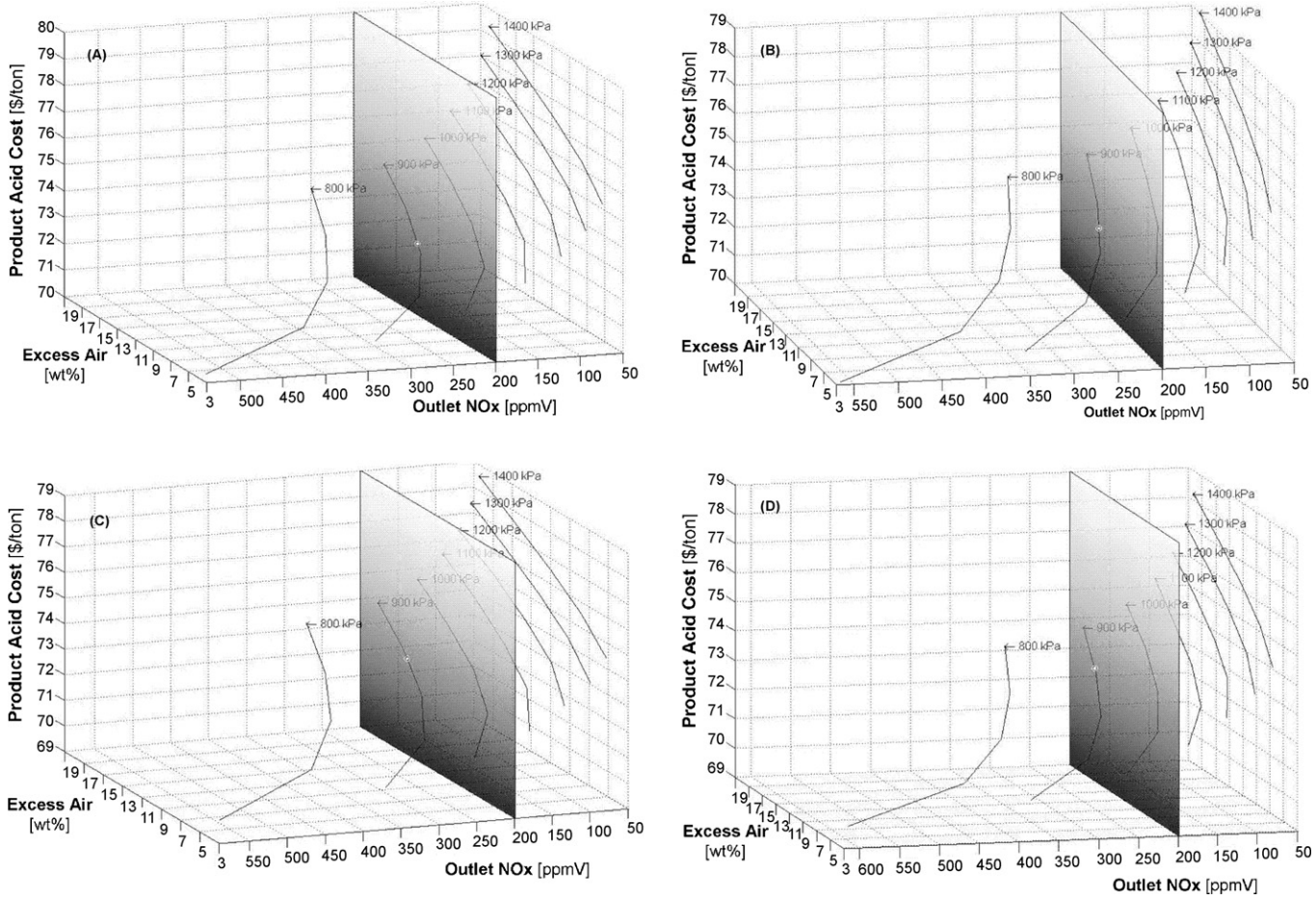

Fig. 9. Optimum operating conditions under constrain of 200 ppmV NO*x* at outlet (60% product quality). Effect of pressure and excess air at chiller zone temperature of 20 °C for: (A) 300 TPD, (B) 310 TPD, (C) 320 TPD, (D) 330 TPD.

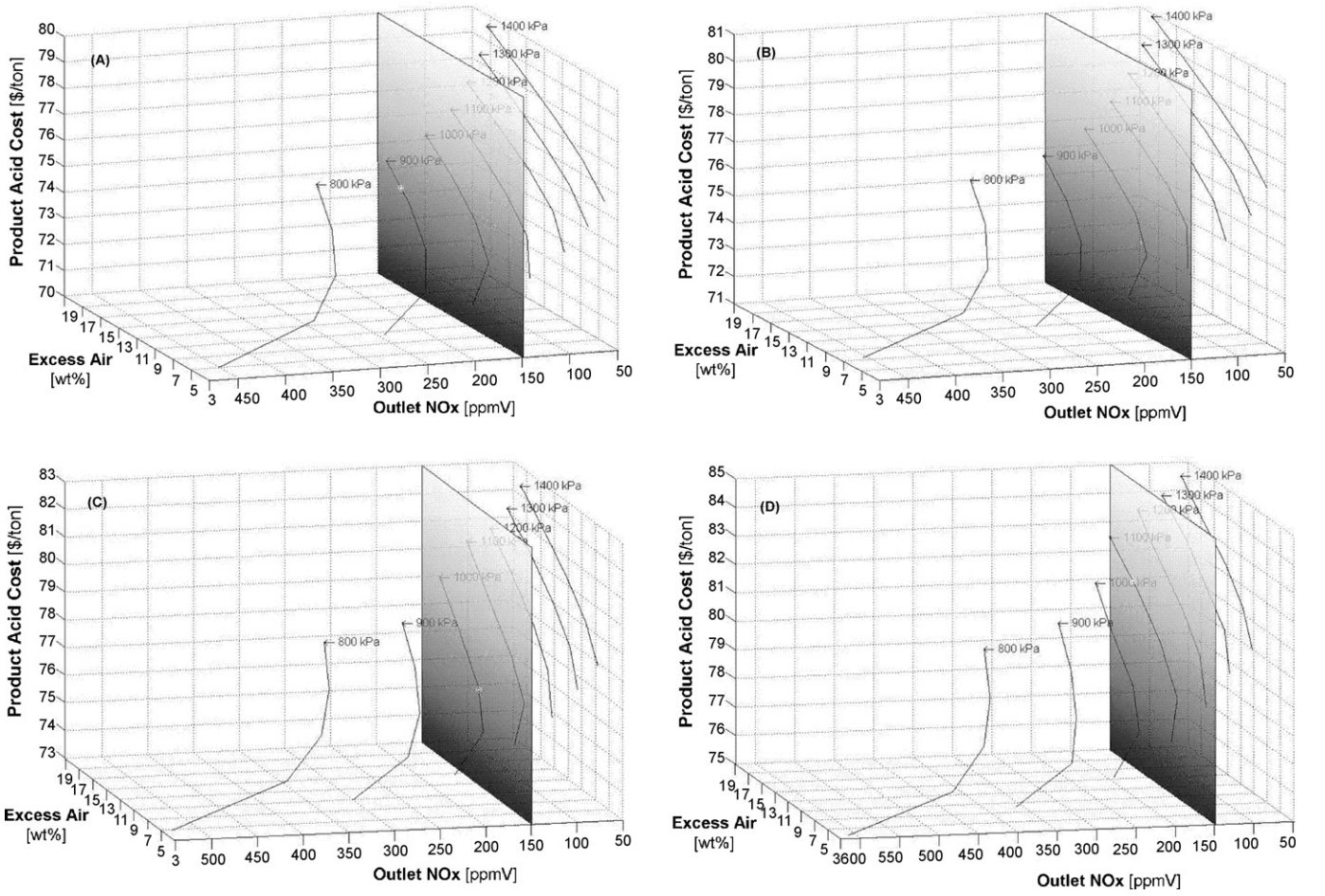

Fig. 10. Optimum operating conditions under constrain of 200 ppmV NO*x* at outlet (300 TPD production 100% HNO_3 basis). Effect of pressure and excess air for: (A) 60%, (B) 61%, (C) 62%, (D) 63%.

absorber tray temperature of 40 °C and constrain of 200 ppmV, outlet NO*x* gives optimum for 300 TPD as 72.40 $/ton operating at 1000 kPa and 5.23% (wt) excess air; for 310 TPD as 72.19 $/ton operating at 1000 kPa and 5.69% (wt) excess air; for 320 TPD as 72.01 $/ton operating at 1000 kPa and 6.13% (wt) excess air; and for 330 TPD as 71.85 $/ton operating at 1000 kPa and 6.54% (wt) excess air.

Therefore when operated at 10 °C instead of 20 °C, reduction in operating cost by 0.28% per ton of product acid is possible; which translates into a profit improvement of 1.20% for 300 TPD plant. Also, when capacity is increased by 10% (to 330 TPD), a reduction in operating cost by 1.02% per ton of product acid, is possible; which translates into a profit enhancement by 14.83% or 1232 $/day.

3.4. Strategy for quality improvement

The market price for various concentration of nitric acid is presented in Table 5.

3.4.1. Effect of outlet NOx concentration

Fig. 10A–D show, as the quality of the HNO_3 increases, for an absorber tray temperature of 40 °C and chiller zone temperature of 10 °C, the production cost per ton of product acid increases. Simulations have been performed for a pressure range of 800–1400 kPa and excess air range of 3–19% (wt). The shaded plane in the figures is the 200 ppmV outlet NO*x* constrain, and the 3D view of the figures shows the operating conditions meeting the constrain. For a 300 TPD, the optimum observed for 60% is 72.20 $/ton operating at 900 kPa and 8.54% (wt) excess air; for 61% is 73.70 $/ton operating at 1000 kPa and 4.12% (wt) excess air; for 62% is 75.31 $/ton operating at 1000 kPa and 5.23% (wt) excess air; and for 63% is 78.10 $/ton operating at 1100 kPa and 3.61% (wt) excess air.

Table 5
Cost of product acids

Product acid quality (wt%)	Product cost ($/ton)
60	90
61	98
62	102
63	107
64	111
66	119
68	131
98	184

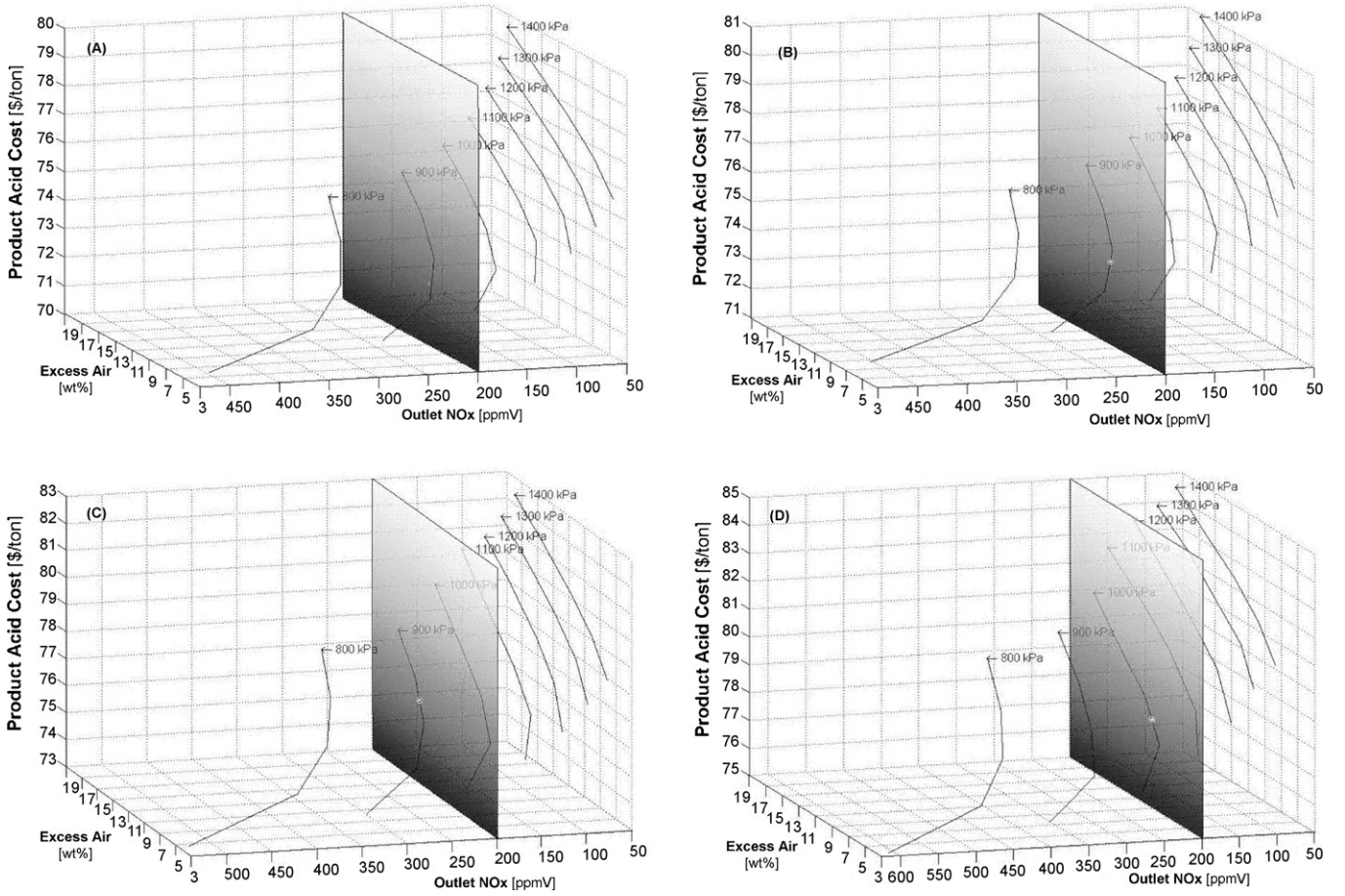

Fig. 11. Optimum operating conditions under constrain of 150 ppmV NO*x* at outlet (300 TPD production 100% HNO_3 basis). Effect of pressure and excess air for: (A) 60%, (B) 61%, (C) 62%, (D) 63%.

Therefore, as quality increases, from 60% to 63% profit enhances by 3550 $/day for 61%, 4514 $/day for 62% and 5362 $/day for 63%.

Fig. 11A–D show, the optimum for constrain of 150 ppmV outlet NO*x*. For 300 TPD, it gives for 60%, 72.79 $/ton operating at 1000 kPa and 6.88% (wt) excess air; for 61%, 74.43 $/ton operating at 1000 kPa and 8.28% (wt) excess air; for 62%, 76.21 $/ton operating at 1100 kPa and 4.87% (wt) excess air; and for 63%, 79.66 $/ton operating at 1200 kPa and 4.93% (wt) excess air. Therefore, for a 50 ppmV reduction in the NO*x* outlet constrain, improvement in profit margin for 61% is 3191 $/day, 62% is 4079 $/day and 63% is 4619 $/day, taking the reference as; 60% product quality at 300 TPD and 200 ppmV outlet NO*x* constrain. The demand on outlet NO*x* constrain will increase the product cost for 60–63%, by 0.8–2.0%. However, daily profit will drop by 10.11% for 61%, 9.64% for 62%, and 13.85% for 63%.

3.4.2. Effect of absorber tray temperature

Fig. 12A–C show the effect of 10 °C rise in absorber tray temperature for various qualities on the cost of production. For 300 TPD and chiller zone temperature of 10 °C, constrain of 200 ppmV outlet NO*x* gives optimum for 60% as 72.96 $/ton operating at 1000 kPa and 4.98% (wt) excess air; for 61% as 74.93 $/ton operating at 1000 kPa and 6.93% (wt) excess air; and for 62% as 78.06 $/ton operating at 1100 kPa and 4.77% (wt) excess air. Therefore, if operated at 40 °C instead of 50 °C, a reduction in operating cost by 1.1% per ton of product acid is possible; which translates into a profit enhancement of 4.74% for 300 TPD plant and 60% product quality. Similarly, for 61% and 62% product quality, by operating at 10 °C higher, loss of profit by 17.04% and 29.47%, respectively is observed with reference to operating 60% product quality at 40 °C absorber tray temperature. Thereby, operating at 40 °C absorber tray temperature, profit enhancement for 61% is 3550 $/day; and for 62% is 4514 $/day; for 300 TPD.

3.4.3. Effect of chiller zone temperature

Fig. 13A–D show, the effect of 10 °C rise in chiller zone temperature for various qualities on cost of production. For absorber tray temperature of 40 °C and constrain of 200 ppmV outlet NO*x* gives optimum for 60% as 72.40 $/ton operating at 1000 kPa and 5.23% (wt) excess air; for 61% as 73.91 $/ton operating at 1000 kPa and 6.08% (wt) excess air; for 62% as 75.57 $/ton operating at 1100 kPa and 7.44% (wt) excess air; and for 63% as 78.49 $/ton operating at 1200 kPa and 6.62% (wt) excess air.

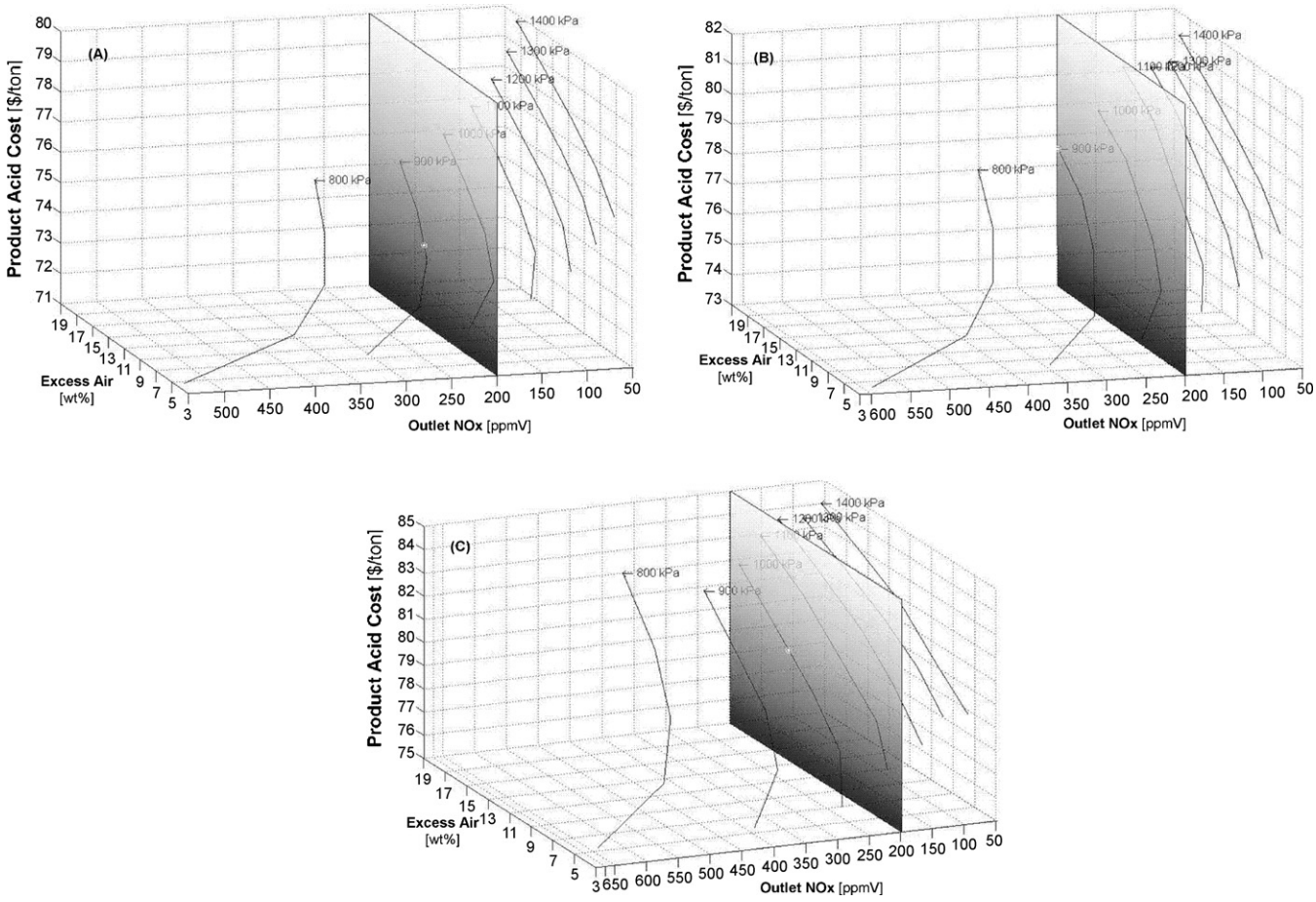

Fig. 12. Optimum operating conditions under constrain of 200 ppmV NO*x* at outlet (300 TPD production 100% HNO_3 basis). Effect of pressure and excess air at absorber tray temperature of 50 °C for: (A) 60%, (B) 61%, (C) 62%.

Therefore when operated at 10 °C instead of 20 °C, a reduction in operating cost by 0.28% per ton of product acid is possible; which translates into a profit improvement of 1.20% for 60% product quality. Also, when the quality is increased, a 10 °C rise in chiller zone temperature reduces profit by 2.90% to 3447 $/day for 61%, by 2.78% to 4389 $/day for 62%, and by 3.47% to 5176 $/day for 63% product quality.

3.4.4. *Effect of oxidizer volume*

The importance of NO*x* composition entering the tray column has been emphasized earlier. Higher concentration of tetravalent NO*x* is always desired for getting higher rates of absorption as well as the possibility of getting higher quality. In this context, the oxidizer volume gains an important role and, therefore, it was thought desirable to understand the sensitivity of the oxidizer volume on the capacity and quality of HNO_3 under otherwise identical conditions.

Fig. 14A–D show, for a 300 TPD and 63% product quality, as the volume is increased from 3.36 m^3 to 23.52 m^3, the cost of production shows a minima at 16.80 m^3 oxidizer volume, where profit enhancement is 5576 $/day, with reference to a 300 TPD plant of 60%, with 3.36 m^3 oxidizer volume. Further, Fig. 15A–D show that for a 330 TPD and 63% product quality, as the volume is varied between 3.36 m^3 and 30.24 m^3, the cost of production shows a minima at 10.08 m^3 and the profit enhancement is 7220 $/day, with reference to a 300 TPD plant of 60%, with 3.36 m^3 oxidizer volume.

As, the oxidizer volume is increased more nitrogen tetraoxide formation takes place, resulting in lower cost of production. However, after a certain oxidizer volume, as seen in the above figures; the cost of oxidizer, though marginal, adds to the cost of production; giving us minima for production cost for a range of oxidizer volumes. The reduction in volume for higher capacity is well understood from the optimum process parameters obtained under constrain of 200 ppmV NO*x* at the outlet. For 300 TPD and 63% product quality the optimum conditions are 1000 kPa and 7.29 wt% excess air; while for 330 TPD and 63% product quality the optimum conditions are 1100 kPa and 9.56 wt% excess air. In both the cases the absorber tray temperature and chiller zone temperature are practically at their optimum of 40 °C and 10 °C, respectively. It is the effect of high pressure that reduces the volume of oxidizer for 330 TPD and 63% product quality. If a similar pressure condition is used for 300 TPD with 63% product quality, though the volume reduces, the cost of production was found to increase gradually, thereby reducing the envisaged enhancement of profit.

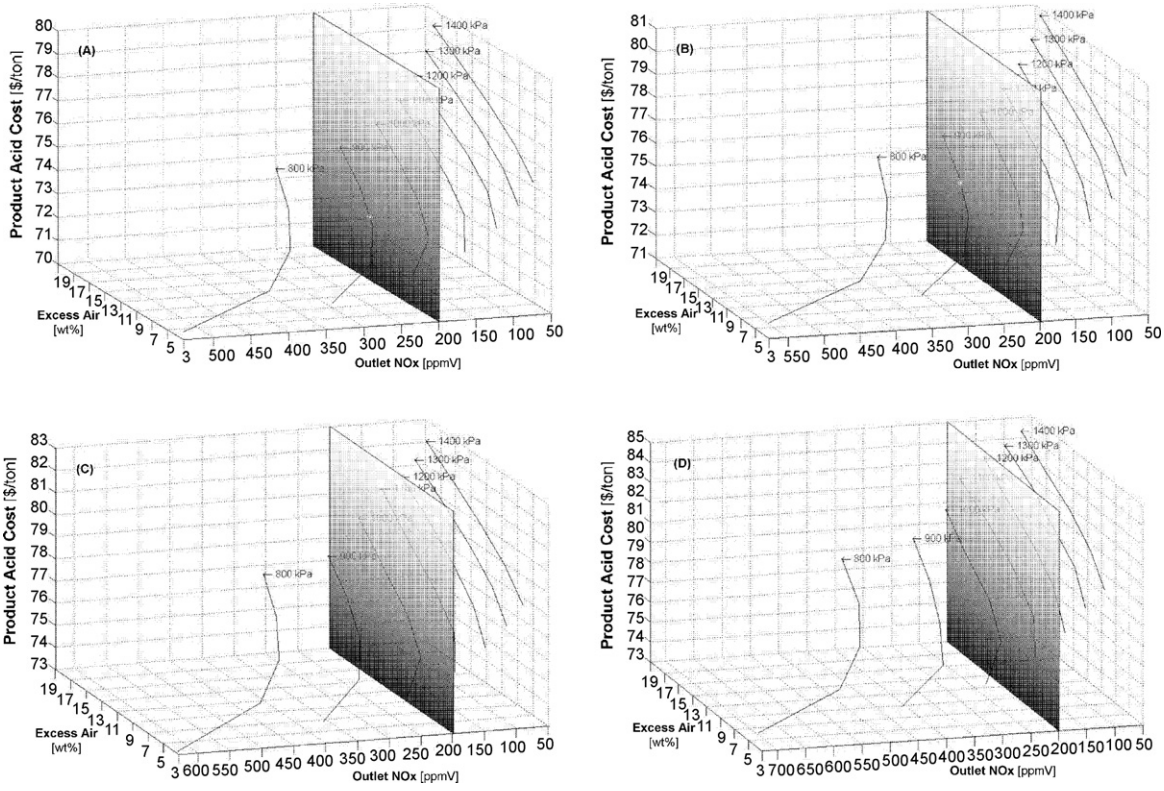

Fig. 13. Optimum operating conditions under constrain of 200 ppmV NO*x* at outlet (300 TPD production 100% HNO_3 basis). Effect of pressure and excess air; at chiller zone temperature of 20 °C for: (A) 60%, (B) 61%, (C) 62%, (D) 63%.

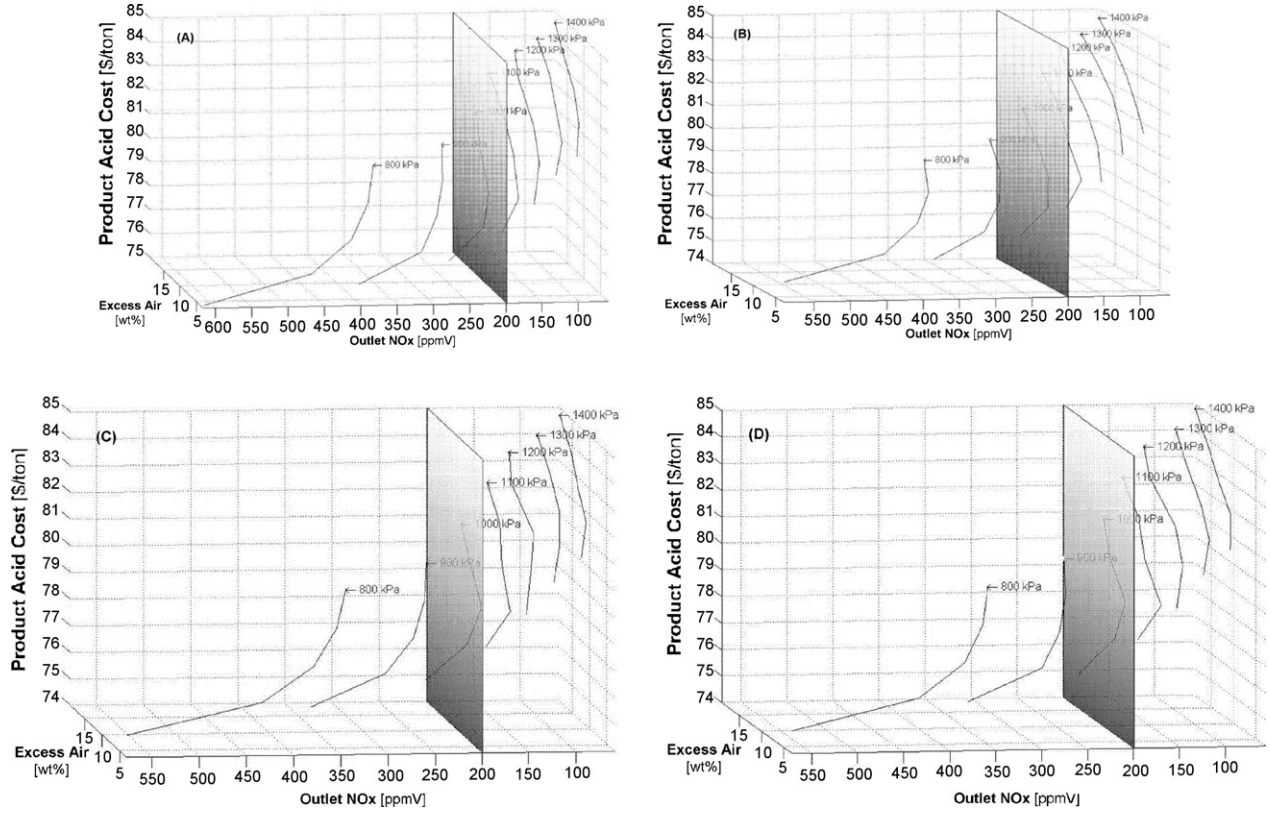

Fig. 14. Optimum operating conditions under constrain of 200 ppmV NO*x* at outlet (300 TPD production 100% HNO_3 basis and 63% product quality). Effect of pressure and excess air; at chiller zone temperature of 10 °C and absorber tray temperature of 40 °C for oxidizer volume: (A) 3.36 m^3, (B) 10.08 m^3, (C) 16.80 m^3, (D) 23.52 m^3.

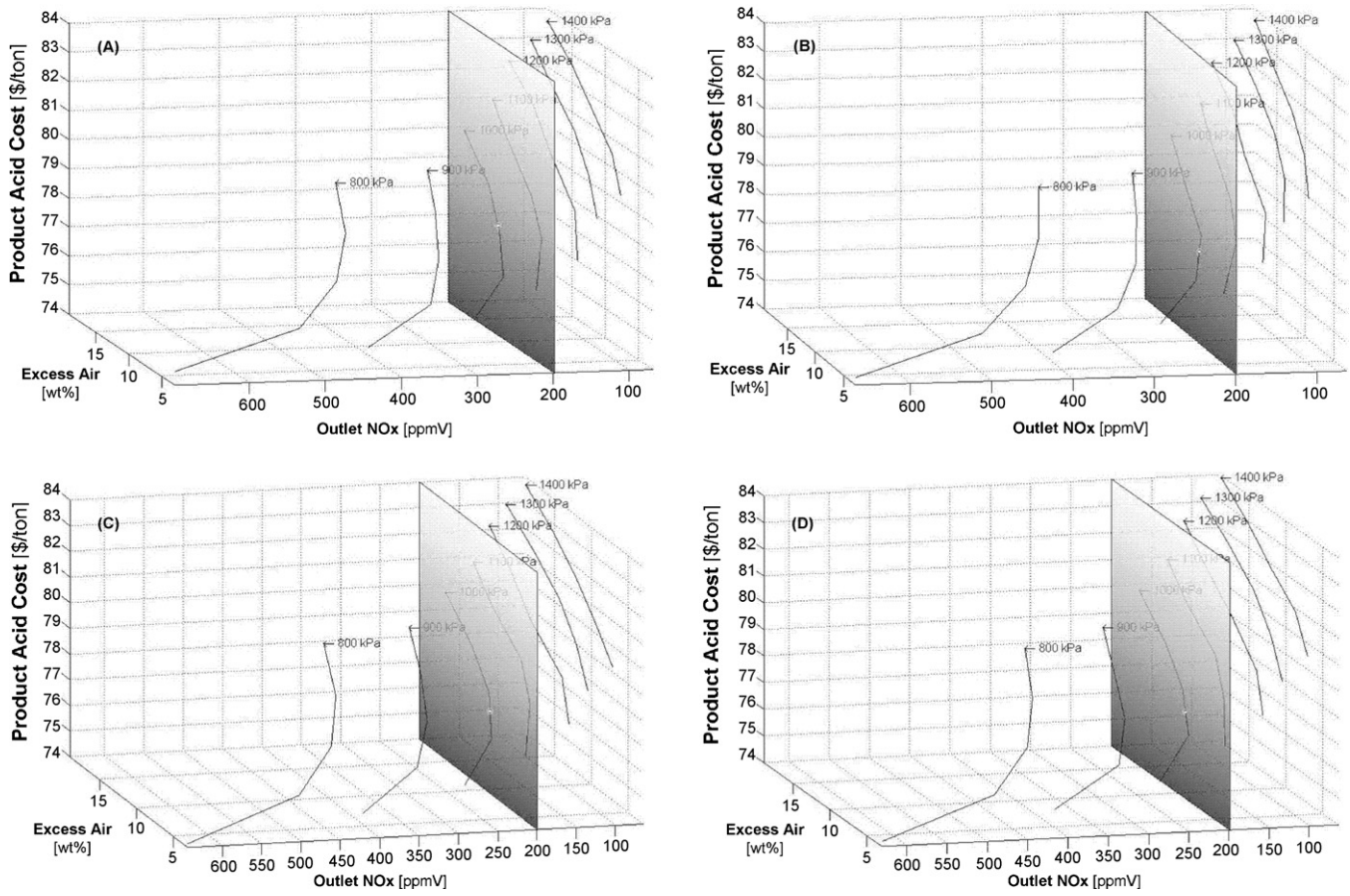

Fig. 15. Optimum operating conditions under constrain of 200 ppmV NOx at outlet (330 TPD production 100% HNO_3 basis and 63% product quality). Effect of pressure and excess air; at chiller zone temperature of 10 °C and absorber tray temperature of 40 °C for oxidizer volume: (A) 3.36 m^3, (B) 10.08 m^3, (C) 16.80 m^3, (D) 30.24 m^3.

4. Conclusions

Models describing important unit operations and unit processes have been presented in earlier section. Additional details of modeling methodology and methods of solution have been outlined in Appendices A and B. For nitric acid plant simulation codes (FORTRAN) have been developed for individual equipment. The data processing was in MATLAB. The important findings of this work are presented below:

(1) The comparison of simulation code predictions with the plant data shows that the predicted plant pressure at four locations (1, 6, 3, and 12 as per Fig. 1) agrees with the plant data within 3.5%. Further, the HNO_3 concentration with respect to tray number was predicted within 5%. These two results validate the simulation codes.
(2) As the constraint on the NOx exit concentration increases, the optimum operating pressure was found to increase. For instance, for a capacity of 330 TPD the optimum pressure for 150 ppmV and 200 ppmV were found to be 1100 kPa and 1000 kPa, respectively.
(3) An increase in the absorber tray temperature was found to demand high pressure or high excess air, to achieve the desired level of NOx at the outlet. Thus for 300 TPD capacity, the optimum for 40 °C and 50 °C were found to be 900 kPa and 8.54 wt% excess air; and 1000 kPa and 4.98 wt% excess air, respectively. However, though optimum pressure for 330 TPD is 1000 kPa for both the temperatures, the excess air requirement was found to increase from 4.80 wt% to 6.33 wt% (the NOx constrain of 200 ppmV remaining the same in all cases).
(4) For the objective of capacity improvement, it was observed that chiller zone temperature has minor influence as compared to the absorber tray temperature. For a 300 TPD capacity, 10 °C decrease in chiller zone and absorber tray temperatures, leads to cost reduction by 0.28% and 1.1%, respectively.
(5) A strategy for capacity improvement has been developed. The optimum conditions to obtain a 330 TPD capacity for 60% product acid under a constrain of 200 ppmV NOx at the outlet, are 1000 kPa, 4.8 wt% excess air, 40 °C absorber tray temperature and 10 °C chiller zone temperature. This was found to result in a cost reduction of 0.74% per ton and profit enhancement of 13.47% per annum, which translates to 1132 $/day profit.
(6) Process parameters like lower outlet NOx concentration, high chiller zone temperature and high absorber tray temperature influence the cost of production and tend to bring

down the achievable profit enhancements, for any desired increment in the quality.

(7) Increasing oxidizer volume to 16.80 m^3 can help in achieving a capacity of 300 TPD with a product quality of 63%. Also, an oxidizer volume of 10.08 m^3 helps in achieving a capacity of 330 TPD with 63% product quality. The effect of pressure is very well observed in these sets of results.

(8) Designing a plant by considering equal divalent nitrogen conversion in the gas space of absorber reduces the optimum product acid cost by 0.25% as compared to a design based on an absorber with equi-spaced plates. Moreover, the optimum design condition obtained by the former method is insensitive to 30% variation in power recovery and 50% variation in fixed capital contribution.

Appendix A

A.1. Oxidizer model

In the oxidizer or pre-conditioning zone, nitric oxide oxidation to nitrogen dioxide takes place in presence of oxygen. As can be observed from Table 1A, the nitric oxide oxidation is accompanied by formation of higher nitrogen oxides and oxy acids. The divalent nitrogen oxide accounts for (i) the unreacted NO, (ii) NO participating in N_2O_3 formation (iii) NO participating in HNO_2 formation; and (iv) NO being formed due to HNO_2 depletion in the as phase.

A.1.1. Oxidizer material balance

Considering plug flow in the oxidizer, the component balances for divalent nitrogen is written as:

$$\frac{dY^*_{NO}}{dz} = -\frac{S}{G}[k_1(p_{NO})^2 p_{O_2}] \tag{1.1}$$

The oxygen depleted in the process is accounted by means of:

$$\frac{dY^*_{O_2}}{dz} = -\frac{1}{2} \times \frac{S}{G}[k_1(p_{NO})^2 p_{O_2}] \tag{1.2}$$

A.1.2. Method of solution

The above Eqs. (1.1) and (1.2), present a boundary value problem. Knowing, the inlet composition of gases entering the oxidizer, the above two equations are solved simultaneously by integrating till exit of the oxidizer, using Runge-Kutta 4th order.

A.1.3. Formation of higher nitrogen oxides

The formation of higher nitrogen oxides reported in Table 1A is computed by considering no formation or removal of reactive nitrogen within a gaseous system, so far phase change is not occurring.

The total number of moles per mole of inert is expressed as:

$$Y_T = Y_{NO} + Y_{NO_2} + Y_{N_2O_3} + Y_{N_2O_4} + Y_{HNO_2} + Y_{HNO_3} + Y_{H_2O} + Y_{O_2} + 1.0 \tag{1.3}$$

The reactive nitrogen per mole of inert is:

$$Y^*_N = Y_{NO} + Y_{NO_2} + 2Y_{N_2O_3} + 2Y_{N_2O_4} + Y_{HNO_2} + Y_{HNO_3} \tag{1.4}$$

The divalent nitrogen per mole of inert is:

$$Y^*_{NO} = Y_{NO} + Y_{N_2O_3} + 0.5Y_{HNO_2} - 0.5Y_{HNO_3} \tag{1.5}$$

The water per mole of inert which accounts for free water vapor and water in form of oxy acids is:

$$Y^*_{H_2O} = Y_{NO} + Y_{N_2O_3} + 0.5Y_{HNO_2} - 0.5Y_{HNO_3} \tag{1.6}$$

The above Eqs. (1.3)–(1.6) can be written in terms of the quantities Y_{NO}, Y_{NO_2} and Y_{H_2O} based on the equilibrium constants for gas phase reactions presented in Table 1A. This will lead to a set of four equations and four unknown terms Y_{NO}, Y_{NO_2}, Y_{H_2O} and Y_T, which can be solved simultaneously, by Newton-Rapson in conjunction with Gauss-Jordan, for known values of Y^*_N, Y^*_{NO}, $Y^*_{H_2O}$, and Y_{O_2}. The values for Y_{HNO_3}, Y_{HNO_2}, $Y_{N_2O_3}$ and $Y_{N_2O_4}$ are evaluated from the equilibrium relations.

Therefore, the oxidizer material balance, coupled with higher nitrogen oxides evaluation through gas equilibria, will give the values of all higher nitrogen oxides at the outlet of an oxidation section.

A.1.4. Oxidizer energy balance

Oxidation of nitric oxide, formation of higher nitrogen oxides and formation of oxy acids in presence of water vapor are all exothermic reactions. The standard heat of reaction are tabulated in Table 1A. Energy balance plays a vital role in oxidation section as it influences the equilibrium constants for the rapid gas phase reactions and also, governs the extent of completion of nitric oxide oxidation.

With the known quantities of component species at the inlet and outlet of the oxidizer section, evaluated from oxidizer material balance and gas equilibria, the heat of formation of various components can be evaluated based on the data presented in Table 1A. The summation of all heats of formations of the individual species over the integration length of the oxidizer will give the heat generated in oxidizer section.

Appendix B

B.1. Absorber model

The absorption on a stage is modeled by dividing the process into two parts (i) the gases bubbling through the pool of liquid, considering it to flow in plug behavior and (ii) the pool of liquid on the stage, considering it to be completely back mixed.

B.1.1. Gases bubbling through liquid

The material balance for the gases bubbling through the pool of liquid is written in terms of:

(a) Divalent nitrogen balance:

$$\frac{dY^*_{NO}}{dz} = -\frac{S}{G}\{k_1(p_{NO})^2 p_{O_2}\varepsilon_G - Ra_{NO,G} + Ra_{N_2O_3,G} + 0.5(Ra_{HNO_2,G} - Ra_{HNO_3,G})\} \quad (2.1)$$

(b) Reactive nitrogen balance:

$$\frac{dY^*_N}{dz} = -\frac{S}{G}\{-Ra_{NO,G} + Ra_{NO_2,G} + 2Ra_{N_2O_3,G} + 2Ra_{N_2O_4,G} + Ra_{HNO_2,G} + Ra_{HNO_3,G}\} \quad (2.2)$$

(c) Water vapor balance:

$$\frac{dY^*_{H_2O}}{dz} = -\frac{S}{G}\{Ra_{H_2O,G} + 0.5Ra_{HNO_2,G} + 0.5Ra_{HNO_3,G}\} \quad (2.3)$$

(d) Oxygen balance:

$$\frac{dY_{O_2}}{dz} = -\frac{1}{2} \times \frac{S}{G}\{k_1(p_{NO})^2 p_{O_2}\varepsilon_G\} \quad (2.4)$$

The point rates of various components in the gas phase is evaluated, based on two film theory, considering mass transfer resistance to be dominant in the gas film. The volumetric rates of gas phase mass transfer are given as:

$$Ra_{NO,G} = (k_G\underline{a})_{NO}(p^i_{NO} - p^o_{NO}) \quad (2.5)$$

$$Ra_{NO_2,G} = (k_G\underline{a})_{NO_2}(p^o_{NO_2} - p^i_{NO_2}) \quad (2.6)$$

$$Ra_{N_2O_3,G} = (k_G\underline{a})_{N_2O_3}(p^o_{N_2O_3} - p^i_{N_2O_3}) \quad (2.7)$$

$$Ra_{N_2O_4,G} = (k_G\underline{a})_{N_2O_4}(p^o_{N_2O_4} - p^i_{N_2O_4}) \quad (2.8)$$

$$Ra_{HNO_2,G} = (k_G\underline{a})_{HNO_2}(p^o_{HNO_2} - p^i_{HNO_2}) \quad (2.9)$$

$$Ra_{HNO_3,G} = (k_G\underline{a})_{HNO_3}(p^o_{HNO_3} - p^i_{HNO_3}) \quad (2.10)$$

$$Ra_{H_2O,G} = (k_G\underline{a})_{H_2O}(p^i_{H_2O} - p^o_{H_2O}) \quad (2.11)$$

In the above Eqs. (2.5)–(2.11), partial pressure of a species in the bulk gas is known, however, the interface partial pressure is unknown. In order to evaluate the interfacial partial pressures, with the help of equilibrium constants, the interface partial pressures are expressed in terms of NO, NO_2, H_2O and HNO_3. Thus, following equations result:

$$p^i_{N_2O_3} = K_3 p^i_{NO}\, p^i_{NO_2} \quad (2.12)$$

$$p^i_{N_2O_4} = K_2(p^i_{NO_2})^2 \quad (2.13)$$

$$p^i_{HNO_2} = (K_4 p^i_{NO} p^i_{NO_2} p^i_{H_2O})^{0.5} \quad (2.14)$$

$$p^i_{HNO_3} = f[T, \text{conc}\,(HNO_3)] \quad (2.15)$$

$$p^i_{H_2O} = f[T, \text{conc}\,(HNO_3)] \quad (2.16)$$

Though the five unknowns of Eqs. (2.5)–(2.11) are now converted to two unknowns (i.e. NO and NO_2) and two known (i.e. HNO_3 and H_2O); still the two unknown values need two simultaneous equations to be evaluated. In order to accomplish this task, the point rates of various components in the liquid phase is evaluated, based on two film theory. The absorption of NO_2, N_2O_3 and N_2O_4 is accompanied by chemical reaction [7]. The volumetric absorption rates for various species are given as:

$$Ra_{NO_2,L} = \underline{a}(H_{NO_2})^{3/2}\left[\frac{2}{3}(kD)_{NO_2}\right]^{1/2}(p^i_{NO_2} - p^b_{NO_2})^{1/2} \quad (2.17)$$

$$Ra_{N_2O_4,L} = \underline{a}(H_{N_2O_4})[(kD)_{N_2O_4}]^{1/2}(p^i_{N_2O_4} - p^b_{N_2O_4}) \quad (2.18)$$

$$Ra_{N_2O_3,L} = \underline{a}(H_{N_2O_3})[(kD)_{N_2O_3}]^{1/2}(p^i_{N_2O_3} - p^b_{N_2O_3}) \quad (2.19)$$

$$Ra_{HNO_2,L} = k_L\underline{a}\,(H_{HNO_2})(p^i_{HNO_2} - p^b_{N_2O_3}) \quad (2.20)$$

Depletion of nitrous acid in the liquid phase leads to evolution of NO; hence, the volumetric rate for NO in the liquid phase is written as:

$$Ra_{NO,L} = \frac{4}{3}Ra_{N_2O_3,L} + \frac{2}{3}Ra_{N_2O_4,L} + \frac{1}{3}Ra_{NO_2,L} + \frac{2}{3}Ra_{HNO_2,L} \quad (2.21)$$

In the above set of Eqs. (2.17)–(2.21), there are eight unknown terms; however three terms can be expressed in terms of NO and NO_2 from Eqs. (2.12)–(2.16). Carberry [11] in his work has shown that for a given set of partial pressures of NO, NO_2 and N_2O_4, there exists a certain limiting concentration of nitric acid beyond which no absorption of N_2O_4 and NO_2 occur; this is heterogeneous equilibrium. Mathematically it is presented in terms of parameter K_6:

$$K_6 = \frac{p^b_{NO}}{(p^b_{N_2O_4})^{1.5}} \quad (2.22)$$

The correlation [29] for the equilibrium constant is:

$$\log_{10} K_H = 30.086 - 0.0693T - (0.197 - 3.27 \times 10^{-4}T)w + 1.227\log_{10}\left[\frac{(100-w)}{w^2}\right] \quad (2.23)$$

For $w < 5\%$ by weight:

$$\log_{10} K_H = 31.96 - 0.0693T + (3.27 \times 10^{-4}T - 0.4193)w \quad (2.24)$$

In the above Eqs. (2.23) and (2.24), K_H is related to partial pressures as:

$$K_H = \frac{p^b_{NO}}{(p^b_{NO_2})^3} = K_2^{1.5}K_6(101.33)^2 \quad (2.25)$$

In order to solve, the two interface partial pressures of NO and NO_2, the following balances are written at the interface;

(a) NO balance at the interface gives:

$$(\mathrm{Ra}_{\mathrm{NO,L}} - \mathrm{Ra}_{\mathrm{NO,G}}) = (\mathrm{Ra}_{\mathrm{N_2O_3,L}} - \mathrm{Ra}_{\mathrm{N_2O_3,G}}) + \frac{1}{2}(\mathrm{Ra}_{\mathrm{HNO_2,L}} - \mathrm{Ra}_{\mathrm{HNO_2,G}}) \quad (2.26)$$

(b) NO_2 balance at the interface gives:

$$(\mathrm{Ra}_{\mathrm{NO_2,G}} - \mathrm{Ra}_{\mathrm{NO_2,L}}) = 2(\mathrm{Ra}_{\mathrm{N_2O_3,L}} - \mathrm{Ra}_{\mathrm{N_2O_3,G}}) + 2(\mathrm{Ra}_{\mathrm{N_2O_4,L}} - \mathrm{Ra}_{\mathrm{N_2O_4,G}}) + \frac{1}{2}(\mathrm{Ra}_{\mathrm{HNO_2,L}} - \mathrm{Ra}_{\mathrm{HNO_2,G}}) \quad (2.27)$$

In the above two Eqs. (2.26) and (2.27), all values from Eqs. (2.5)–(2.21) are substituted to finally get two equations and two unknowns p^i_{NO} and $p^i_{NO_2}$, which are solved using Newton-Rapson in conjunction with Gauss-Jordan. Now, since NO desorbs rapidly from the liquid to the bulk gas, hence,

$$p^i_{NO} = p^b_{NO} \quad (2.28)$$

With the aid of Eqs. (2.28), (2.22) and (2.25) all, heterogeneous equilibrium pressure values are evaluated and Eqs. (2.12)–(2.16) helps to evaluate the interfacial partial pressure values. This will enable in solving Eqs. (2.5)–(2.11), which will finally help us evaluate the Eqs. (2.1)–(2.4). The Y^*_N, Y^*_{NO}, $Y^*_{H_2O}$, and Y_{O_2} thus evaluated will help us get the compositions of the various gas species, by following the gas equilibria solving procedure described in Appendix A.

B.1.2. Liquid pool on a tray

With the evaluations of all components in gas phase at inlet and outlet of the stage, the reactive nitrogen balance in the liquid for the stage is:

$$G(Y^*_{N,n-1} - Y^*_{N,n}) = L_n X^*_{N,n} - L_{n+1} X^*_{N,n+1} \quad (2.29)$$

B.1.3. Absorber energy balance

With the known rates of volumetric mass transfer in gas phase from Eqs. (2.5)–(2.11) and volumetric absorption in liquid phase from Eqs. (2.17)–(2.21), the heat of transfer on an absorber stage can be evaluated from the tabulated data in Table 1B. The heat transfer on every stage is then summed up for the total number of stages in the column.

References

[1] R.E. Kirk, D.F. Othmer, Kirk Othmer Encyclopedia of Chemical Technology, John Wiley and Sons, New York, 1981.

[2] P.J. Hoftizer, F.J.G. Kwanten, in: G. Nonhabel (Ed.), Absorption of Nitrous Gases, Gas Purification Processes for Air Pollution Control, Newnes Butterworths, London, 1972.

[3] C. Matassa, E. Tonca, Basic Nitrogen Compounds, Chemical Publishing Co., New York, 1973.

[4] T.K. Sherwood, R.L. Pigford, C.R. Wilke, Mass Transfer, McGraw-Hill, New York, 1975.

[5] J.J. Carberry, Chemical and Catalytic Reaction Engineering, McGraw Hill, New York, 1976.

[6] G.D. Honti, in: Keleetic (Ed.), Various Processes for the manufacture of commercial grade nitric acid, Nitric Acid and Nitrates—Fertilizer science and Technology Series, Marcel Dekker, New York and Basel, 1985.

[7] J.B. Joshi, V.V. Mahajani, V.A. Juvekar, Absorption of NO*x* gases, Chem. Eng. Commun. 33 (1985) 1–92.

[8] R.M. Counce, J.J. Perona, A mathematical model for nitrogen oxide absorption in a sieve plate column, Ind. Eng. Chem. Process. Design Dev. 19 (1980) 426–431.

[9] D.N. Miller, Mass transfer in nitric acid absorption, AIChE J. 33 (1987) 1351–1357.

[10] W. Weisweiler, K. Eidam, M. Thiemann, E. Scheibler, K.W. Wieand, Absorption of NO/NO_2 in nitric acid, Chem. Eng. Technol. 13 (1990) 97–101.

[11] J.J. Carberry, Some remarks on chemical equilibrium and kinetics in the nitrogen dioxide-water system, Chem. Eng. Sci. 9 (1959) 189–194.

[12] Ir.A.P. Oele, Technological aspects of the catalytic combustion of ammonia with platinum gauze elements, Chem. Reaction Eng., Meeting European Federation Chemical Engineers, 12th, Amsterdam, 1957, pp. 146–157.

[13] V. Fila, B. Bernauer, A mathematical model of a gauze reactor for the ammonia oxidation, Collect. Czech. Chem. Commun. 59 (1994) 855–874.

[14] C.N. Satterfield, D.H. Cortez, Mass transfer characteristics of woven wire screen catalysts, Ind. Eng. Chem. Fundam. 9 (1970) 613–620.

[15] J.C. Armour, J.N. Cannon, Fluid flow through woven screens, AIChE J. 14 (1968) 415–420.

[16] W. Crookes, The volatility of metals of the platinum group, Proc. R. Soc. A86 (1912) 461–477.

[17] C.B. Alcock, G.W. Hooper, Thermodynamics of the gaseous oxides of the platinum group metals, Proc. R. Soc. A254 (1960) 551–561.

[18] G.R. Gillespie, R.E. Kenson, Catalyst system for oxidation of ammonia to nitric acid, Chem. Technol. (1971) 627–632.

[19] M. Pszonicka, Rhodium oxide formation on the surface of Pt-Rh gauzes used in the catalytic oxidation of ammonia, J. Catal. 56 (1979) 472–474.

[20] R.W. Bartlett, Platinum oxidation kinetics with convective diffusion and surface reaction, J. Electrochem. Soc. 114 (1967) 547–550.

[21] D.Q. Kern, Process Heat Transfer, McGraw Hill, New York, 1950.

[22] K. Sadik, L. Hongtan, Heat Exchanger Selection, Rating and Thermal Design, second ed., CRC Press, 2002.

[23] HEDH, Thermal and hydraulic design of heat exchangers, vol. 3, Hemisphere Publishing Co., 1983.

[24] R.W. King, J.C. Fielding, A graphical design method for nitric acid absorption towers, Trans. Inst. Chem. Eng. 38 (1960) 71–82.

[25] V. Sobotka, Modeling of an absorption column for nitric acid manufacture, Int. Chem. Eng. 13 (1973) 718–727.

[26] G. Emig, K. Wohlfahrt, U. Hoffmann, Absorption with simultaneous complex reactions in both phases, demonstrated by the modeling and calculation of a counter current flow column for the production of nitric acid, Comp. Chem. Eng. 3 (1979) 143–150.

[27] F.T. Shadid, D. Handley, Absorption of nitrogen oxides using a baffle tray, Chem. Eng. Res. Dev. 67 (1989) 185–192.

[28] N.J. Suchak, J.B. Joshi, Simulation and optimization of NO*x* absorption system in nitric acid manufacture, AIChE J. 40 (1994) 944–956.

[29] M.P. Pradhan, N.J. Suchak, P.R. Walse, J.B. Joshi, Multicomponent gas absorption with multiple reactions: modeling and simulation of NO*x* absorption in nitric acid manufacture, Chem. Eng. Sci. 52 (1997) 4569–4591.

[30] N.J. Suchak, K.R. Jethani, J.B. Joshi, Modeling and simulation of NO*x* absorption in pilot-scale packed columns, AIChE J. 37 (1991) 323–339.

[31] E. Decanini, G. Nardini, A. Paglianti, Absorption of nitrogen oxides in columns equipped with low-pressure drops structured packings, Ind. Eng. Chem. Res. 39 (2000) 5003–5011.

[32] B. Hupen, E.Y. Kenig, Rigorous modeling of NO*x* absorption in tray and packed columns, Chem. Eng. Sci. 60 (2005) 6462–6471.

[33] M.M. Sharma, R.A. Maheslkar, V.D. Mehta, Mass transfer in plate columns, Brit. Chem. Eng. 14 (1969) 37–43.

[34] E.E. Ludwig, Applied Process Design for Chemical and Petrochemical Pants, vol. 3, second ed., Gulf Publishing Company, 1983.